Insight into Notch Signaling Steps That Involve *pecanex* from Dominant-Modifier Screens in *Drosophila*

Tomoko Yamakawa,*,[1] Yu Atsumi,[†] Shiori Kubo,* Ami Yamagishi,* Izumi Morita,* and Kenji Matsuno*,[1]
*Department of Biological Sciences, Graduate School of Science, Osaka University, Toyonaka 560-0043, Japan and [†]Department of Biological Science and Technology, Graduate School of Industrial Science and Technology, Tokyo University of Science, 125-8585, Japan

ABSTRACT Notch signaling plays crucial roles in intercellular communications. In *Drosophila*, the *pecanex* (*pcx*) gene, which encodes an evolutionarily conserved multi-pass transmembrane protein, appears to be required to activate Notch signaling in some contexts, especially during neuroblast segregation in the neuroectoderm. Although Pcx has been suggested to contribute to endoplasmic reticulum homeostasis, its functions remain unknown. Here, to elucidate these roles, we performed genetic modifier screens of *pcx*. We found that *pcx* heterozygotes lacking its maternal contribution exhibit cold-sensitive lethality, which is attributed to a reduction in Notch signaling at decreased temperatures. Using sets of deletions that uncover most of the second and third chromosomes, we identified four enhancers and two suppressors of the *pcx* cold-sensitive lethality. Among these, five genes encode known Notch-signaling components: *big brain*, *Delta* (*Dl*), *neuralized* (*neur*), *Brother of Bearded A* (*BobA*), a member of the *Bearded* (*Brd*) family, and *N-ethylmaleimide-sensitive factor 2* (*Nsf2*). We showed that *BobA* suppresses Dl endocytosis during neuroblast segregation in the neuroectoderm, as *Brd* family genes reportedly do in the mesoderm for mesectoderm specification. Analyses of *Nsf2*, a key regulator of vesicular fusion, suggested a novel role in neuroblast segregation, which is distinct from Nsf2's previously reported role in imaginal tissues. Finally, *jim lovell*, which encodes a potential transcription factor, may play a role in Notch signaling during neuroblast segregation. These results reveal new research avenues for Pcx functions and Notch signaling.

KEYWORDS *pecanex*; *Drosophila melanogaster*; dominant modifier screen; Delta-Neuralized-Bearded pathway; Notch signaling

CELL signaling via the Notch receptor is an evolutionarily conserved mechanism that mediates local cell–cell communications required for development and homeostasis in metazoans (Artavanis-Tsakonas *et al.* 1999; Cau and Blader 2009; Kopan and Ilagan 2009). Notch signaling plays essential roles in many biological events, including cell-fate decisions, pattern formation, and the regulation of cell physiology (Kim *et al.* 1996; Palmeirim *et al.* 1997; Bessho and Kageyama 2003; Le Bras *et al.* 2011; Guruharsha *et al.* 2012). Therefore, defects in Notch signaling are associated with various human diseases, such as leukemia, cancers, cerebral infarction, Alagille syndrome, and multiple sclerosis (Ellisen *et al.* 1991; Joutel *et al.* 1997; Li *et al.* 1997; John *et al.* 2002; Nicolas *et al.* 2003). The molecular mechanisms of Notch signaling have been extensively studied, and its main process is well understood (Kopan and Ilagan 2009; Guruharsha *et al.* 2012). However, various additional Notch-signaling components continue to be identified through a wide range of genetic and biochemical studies (Artavanis-Tsakonas *et al.* 1995; Bray 2016). In many cases, the specific roles of these components remain elusive, although they are required for Notch signaling activation or regulation at least in some contexts. Understanding the functions of these factors will help elucidate the detailed mechanisms of Notch signaling, and could lead to new therapeutic strategies for Notch pathway-related human diseases.

The Notch receptor family consists of transmembrane proteins containing up to 36 epidermal growth factor-like repeats in their extracellular domain (Wharton *et al.* 1985). In

doi: https://doi.org/10.1534/genetics.118.300935
Manuscript received March 19, 2018; accepted for publication May 22, 2018; published Early Online May 31, 2018.
Supplemental material available at Figshare: https://doi.org/10.6084/m9.figshare.6395831.
[1]Corresponding authors: Department of Biological Sciences, Graduate School of Science, Osaka University, 1-1 Machikaneyama, Toyonaka, Osaka 560-0043, Japan. E-mail: tyamakawa@bio.sci.osaka-u.ac.jp; and kmatsuno@bio.sci.osaka-u.ac.jp

the endoplasmic reticulum (ER) or Golgi, Notch undergoes post-translational modifications such as *N*-glycosylation, *O*-fucosylation, and *O*-glucosylation (Bruckner *et al.* 2000). The Notch extracellular domain is then cleaved by Furin (S1 cleavage), and the processed Notch fragments rebind to each other within the Golgi (Logeat *et al.* 1998; Kidd and Lieber 2002; Lake *et al.* 2009). At the cell surface, Notch binds to Delta- or Serrate-type ligands that are presented on the surface of neighboring cells (Fehon *et al.* 1990; Rebay *et al.* 1991). The extracellular domain of Notch is mechanically pulled by the ligands; this pulling is achieved by ligand endocytosis, which requires ubiquitination of the ligands by Neuralized and Mindbomb (Wang and Struhl 2005; Meloty-Kapella *et al.* 2012). The pulling force induces a conformational change in the Notch extracellular domain, leading to its cleavage at the juxta-membrane region by Kuzbanian/ADAM10 (S2 cleavage) (Stephenson and Avis 2012). Subsequently, the membrane-tethered Notch intracellular domain is cleaved within the transmembrane domain by γ-secretase (S3 cleavage), which releases the Notch intracellular domain from the membrane (Struhl *et al.* 1993; Mumm and Kopan 2000). The Notch intracellular domain is then translocated to the nucleus, where it functions as a coactivator of transcription, leading to the promoter activation of various target genes, such as *Enhancer of split* [*E*(*spl*)] in *Drosophila* (Bailey and Posakony 1995).

In *Drosophila*, in addition to the core components of Notch signaling, several other genes have also been identified as components of the Notch signaling pathway, although the roles of their products remain to be clarified (Hori *et al.* 2013). One such gene is *pecanex* (*pcx*). Embryos homozygous or hemizygous for *pcx* lacking its maternal contribution (pcx^{mz}) exhibit neural hyperplasia, termed the neurogenic phenotype (Perrimon *et al.* 1984); this phenotype is considered evidence for the depletion of Notch signaling (Simpson 1990). Thus, *pcx* is a maternal neurogenic gene. In addition, the expression of *E*(*spl*) *m8* and *single-minded*, which are target genes of Notch signaling, is reduced in pcx^{mz} embryos (Yamakawa *et al.* 2012). Therefore, *pcx* is essential for Notch signaling, at least in certain contexts, such as in neuroblast segregation, which occurs through lateral inhibition in the neuroectoderm. *pcx* encodes an ER-resident multi-pass transmembrane protein that consists of 3433 amino acids and is highly conserved from *Drosophila* to humans (LaBonne *et al.* 1989). In addition to the neurogenic phenotype, ER enlargement is observed in a subset of cells in pcx^{mz} embryos (Yamakawa *et al.* 2012). Both the neurogenic phenotype and the ER defects of pcx^{mz} embryos are rescued through ectopic induction of the unfolded protein response, which promotes ER functions such as protein folding (Kaufman 1999; Yamakawa *et al.* 2012). These findings suggest that Pcx is required for normal functions of the ER, which are essential for activating Notch signaling (Yamakawa *et al.* 2012). However, the biochemical functions of Pcx in Notch signaling remain unclear.

We considered that a genetic modifier screen might be a useful approach for obtaining additional insights into the function of *pcx*. Genetic modifier screens have been used in various organisms including *Drosophila* to identify genes functioning in a common biochemical pathway (St Johnston 2002). Genetic modifiers identified by such screens can be informative for deducing the function of the affected gene. Such information might be particularly valuable in the case of *pcx*, given that Pcx does not carry any protein motifs that suggest its biochemical functions (Gilbert *et al.* 1992). Thus, in this study, we performed genetic screens to identify dominant modifiers of a cold-sensitive lethality that is associated with the *pcx* mutation condition. The dominant enhancers and suppressors of *pcx* identified from the screens provide insight into the steps of the Notch signaling cascade where *pcx* might be involved.

Materials and Methods

Fly strains and genetics

A standard *Drosophila* medium was used. The culture was maintained at 25° unless otherwise stated. Canton-S was used as the wild-type strain. The mutants used were: pcx^{3}, a hypomorphic allele (Mohler 1977; Mohler and Carroll 1984); $big\ brain^{1}$ (bib^{1}), a null allele (Lehmann *et al.* 1981); $Delta^{5F102}$(Dl^{5F102}), a loss-of-function allele (Vässin and Campos-Ortega 1987); $jim\ lovell^{47}$ (lov^{47}), a hypomorphic allele lacking a 1.4-kb sequence upstream of *lov* (a gift from Dr. Kathleen Beckingham; Bjorum *et al.* 2013); $neuralized^{1}$ ($neur^{1}$), a loss-of-function allele (Leviten and Posakony 1996); and $N\text{-}ethylmaleimide\text{-}sensitive\ factor\ 2^{A15}$ ($Nsf2^{A15}$), a hypomorphic allele (Mahoney *et al.* 2006). Deficiency (Df) kits used for the initial screens were obtained from the Bloomington *Drosophila* Stock Center (BDSC) (Cook *et al.* 2012). Small-Df strains that uncovered smaller parts of the regions deleted in the original Dfs included in the Df kits were also obtained from BDSC. Furthermore, 30 additional small Dfs that uncovered the gap regions of the Df kits used for the initial screens were also provided by BDSC. *Df*(*2R*)*gsb* and $Df(2R)GGG^{d13}$ were kindly provided by Markus Noll (He and Noll 2013).

Determination of pupa and eclosed fly numbers under the cold-sensitive lethality of pcx/+^{m}

To characterize the cold-sensitive lethality, which provides a useful assay for *pcx* function in our genetic screens and in our characterization of mutants identified from the screens, we scored the numbers of pupae and eclosed flies. Five *pcx* homozygous or wild-type (control) virgin females were mated with five wild-type males in plastic vials containing a standard *Drosophila* medium. The cultures were maintained at 18, 25, and 28° for 18 days, and then the pupae and/or adult female progenies were counted. The male progenies obtained from *pcx* homozygous females (pcx/Y^{m}) are known to be embryonic lethal (Yamakawa *et al.* 2012). The number of female wild-type pupae was deduced by assuming that half of the total pupae were female (Figure 1B). The eclosed

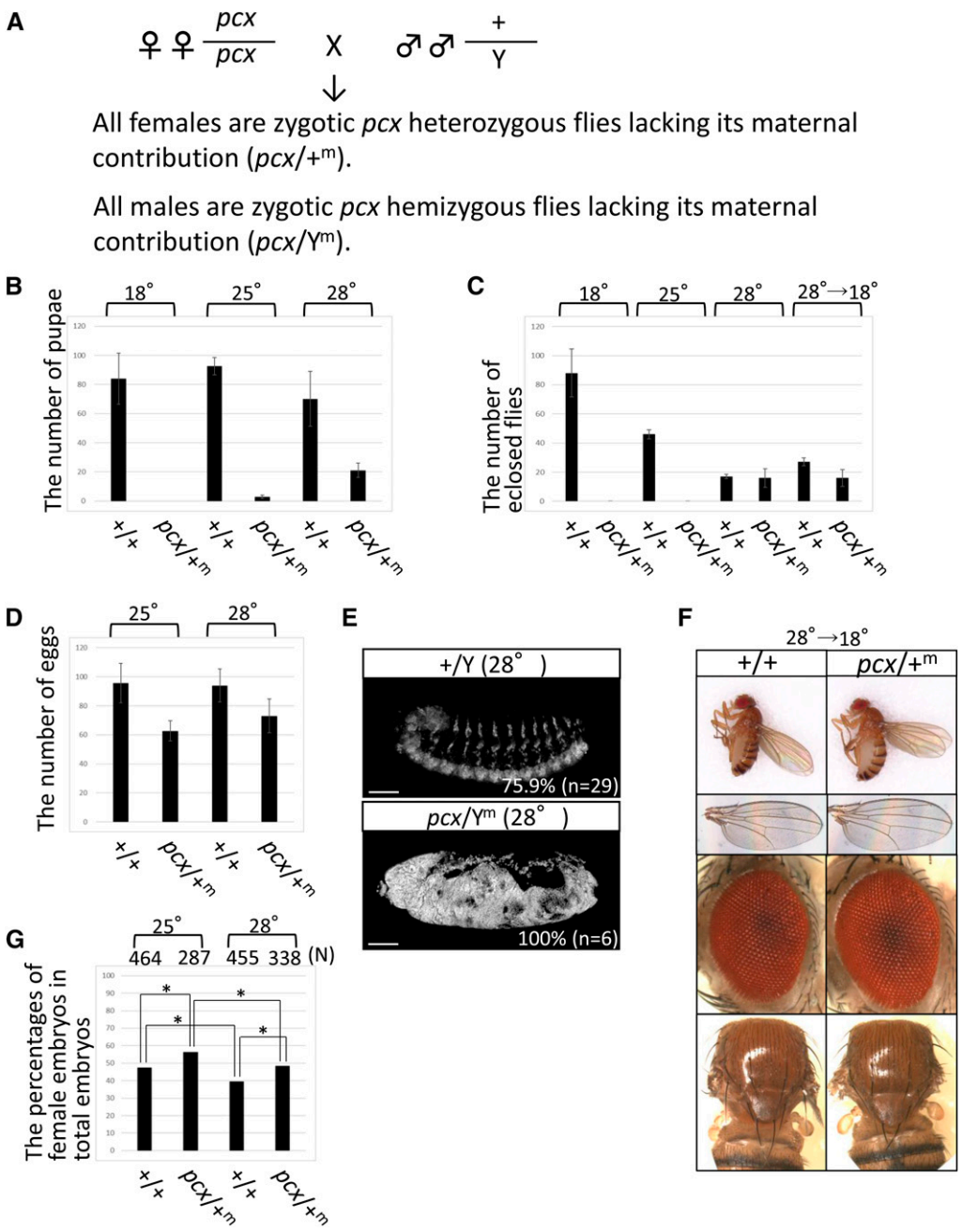

Figure 1 *pcx* exhibits cold-sensitive lethality. (A) Mating scheme to analyze the cold-sensitive lethality of *pcx*/+^{m}. Five *pcx* homozygous females were mated with wild-type males. All females of the F1 progeny were *pcx* heterozygotes lacking maternal *pcx* (*pcx*/+^{m}) and exhibited cold-sensitive lethality. All males of the F1 progeny were *pcx* hemizygotes lacking maternal *pcx* (*pcx*/Y^{m}) and exhibited embryonic lethality. (B) Numbers of wild-type female (+/+, 50% of pupae were predicted to be female) and *pcx*/+^{m} (F1 female) pupae cultured at 18, 25, or 28°. SD are indicated. (C) Numbers of wild-type female (+/+) and *pcx*/+^{m} (F1 female) adults obtained from cultures at 18, 25, or 28° or cultures with a temperature shift from 28 to 18°. In the temperature-shift experiment, the cultures were maintained at 28° until third-instar larvae appeared, and then they were maintained at 18° for 18 days in total. SD are indicated. (D) Numbers of wild-type female (+/+) and *pcx*/+^{m} (F1 female) eggs at 25 and 28°. Sex of embryos was determined by anti-Sxl antibody staining. SD are indicated. (E) Lateral views of wild-type (+/Y) and *pcx*^{mz} (*pcx*/Y^{m}) embryos cultured at 28° and immunostained with a neuron-specific antibody (anti-Elav antibody) at stage 13–14. These embryos were identified as males based on the absence of anti-Sxl antibody staining. (F) Phenotypes of wild-type (+/+) and *pcx*/+^{m} adults cultured with the temperature shift from 28 to 18°. From top to bottom, adult females, wings, eyes, and thoraxes. (G) Percentage of total embryos cultured at 25 or 28° that were female embryos (+/+ and *pcx*/Y^{m}). The number of total embryos examined is shown as (N) at the top. * $P > 0.01$, ** $P < 0.01$.

females were identified by their female genitalia and counted (Figure 1C and Figure 5, A–C). These experiments were performed in triplicate. For the temperature-shift analysis in Figure 1, C and F, the parental flies were maintained at 28° until third-instar larvae appeared, and then the cultures were maintained at 18°. In Figure 5, A–C, to evaluate the dominant modifiers identified in the screens, genotypes of the female adults were determined by the absence of appropriate balancer chromosomes (*CyO* or *TM3*); otherwise, the same procedures were used.

Measurement of egg numbers

The number of eggs laid by wild-type and *pcx* homozygous females was counted (Figure 1D). Five *pcx* homozygous or wild-type virgin females were mated with five wild-type males in a 50-ml tube containing a glass plate with grape agar

and yeast paste. Eggs were collected for 48 hr, with four replacements of the glass plate, at 25 or 28°.

Determination of female embryo percentage

The percentage of female embryos was analyzed (Figure 1G). Five *pcx* homozygous or wild-type virgin females were mated with five wild-type males in a 50-ml tube containing a glass plate with grape agar and yeast paste. Eggs were collected for 48 hr with four replacements of the glass plate, at 25 or 28°. The vitellin membrane of the eggs was removed by heptane-methanol emulsion. Remaining vitellin membrane was removed from embryos with a tungsten needle after placing the embryos on a piece of double-sided tape covered with PBT (137 mM NaCl, 10 mM Na_2HPO_4, 2.7 mM KCl, 1.8 mM KH_2PO_4, 10% TritonX100, pH 7.4). The embryos were then stained with a female-specific anti-Sexlethal (Sxl) antibody (Bopp *et al.* 1991), and the percentage of female embryos was determined. Experiments were performed in triplicate. Statistical significance was determined by the chi-square test.

Measurement of hatching rate

The percentage of female eggs from which first-instar larvae successfully hatched was determined as the hatching rate (Figure 2A). Five *pcx* homozygous or wild-type virgin females were mated with five wild-type males in a 50-ml tube containing a glass plate with grape agar and yeast paste. Eggs were collected for 48 hr with four replacements of the glass plate, and then incubated for another 3 days, at 25 or 28°. The number of female eggs was deduced by assuming that half of the total number of eggs were female. The number of wild-type female larvae was deduced using the same assumption. All of the first-instar larvae obtained from *pcx* homozygous females were female (*pcx*/+^{m}).

Measurement of the rate of survival to the third-instar larval stage

In Figure 2B and Figure 5, D–F, the rate of survival to the third-instar larval stage was determined. The rate of survival to the third-instar larval stage is the number of female third-instar larvae with the indicated genotype divided by the deduced total number of female embryos with that genotype (×100). Five *pcx* homozygous or wild-type virgin females were mated with five wild-type males in a 50-ml tube containing a glass plate with grape agar and yeast paste. Eggs were collected as described above and the total eggs were counted. The number of eggs with each genotype was estimated based on Mendel's laws and the sex ratio. All of the hatched larvae were transferred to the standard medium and cultured at 25 or 28°. Thereafter, the sex of all larvae was determined by observing the gonad size at the third-instar larval stage. In addition, the presence of dominant modifiers in heterozygotes was determined by the absence of appropriate balancer chromosomes, judged by β-galactosidase (LacZ) staining (Kozlova *et al.* 1998). Experiments were performed in triplicate. The statistical significance of the survival rate to the third instar larval stage was examined by the chi-square test.

Measurement of pupation and eclosion rates

To analyze the lethality of *pcx*/+^{m} females from the third-instar larval to pupal stages, we calculated the "pupation rate," which is the number of pupating females divided by the number of collected third-instar larvae (×100). The sex was determined at this stage based on the gonad size (Figure 2C). The *pcx*/+^{m} and wild-type larvae were collected as described above.

To determine the lethality of *pcx*/+^{m} females during eclosion, we also calculated the "eclosion rate," which was the number of eclosed females divided by the number of pupae (×100) (Figure 2D). The sex of pupae was determined at the third-instar larval stage, as described above. Experiments were performed in triplicate. The statistical significance of the pupation and eclosion rates was examined by the chi-square test.

Dominant modifier screens based on the cold-sensitive phenotype of pcx/+^{m}

Df kits of the second and third *Drosophila* chromosomes were used for the dominant modifier screens (Cook *et al.* 2012) (Supplemental Material, Table S1). Together, the Df kits cover ~98% of the genome in each chromosome (Cook *et al.* 2012). In addition, to fill in the gaps of the Df kits, we picked 30 available small Dfs located in the gaps of the primary Dfs (Table S2) and subjected them to the same screens. For the initial screens, five *pcx* homozygous virgin females were mated with five wild-type (control) or Df/Balancer males and cultured at 25 or 28°. At 25°, the Dfs were evaluated as positive when the subsequent generations without Balancers (*pcx*/+; Df/+ embryos lacking maternal *pcx*) eclosed (>10 adults), while the control progenies (*pcx*/+; +/+ lacking maternal *pcx*) were virtually embryonic lethal (no adults) under the same conditions. These deficiencies represented dominant suppressors of the *pcx*/+^{m} lethality, and potential genes encoding negative regulators of *pcx* might exist in the genomic regions uncovered therein. At 28°, the Dfs were evaluated as positive if *pcx*/+; Df/+ flies lacking maternal *pcx* failed to eclose (no adults), while the control progenies (*pcx*/+; +/+ lacking maternal *pcx*) developed to adulthood (>10 adults). These deficiencies represented dominant enhancers of the lethality, and potential genes positively acting in conjunction with *pcx* might exist in the respective uncovered genomic regions.

To identify the dominant modifiers as single loci, smaller deficiencies that uncovered smaller parts of the genomic regions deleted in the Dfs identified in the first screens were subjected to the same analyses. After defining the minimal genomic regions that encompassed the loci responsible for the dominant modifications of the *pcx* lethal phenotypes, we searched for genes known to be involved in Notch signaling within these minimal regions. This mapping analysis using Dfs suggested that the *Brother of bearded A* (*BobA*) gene was a

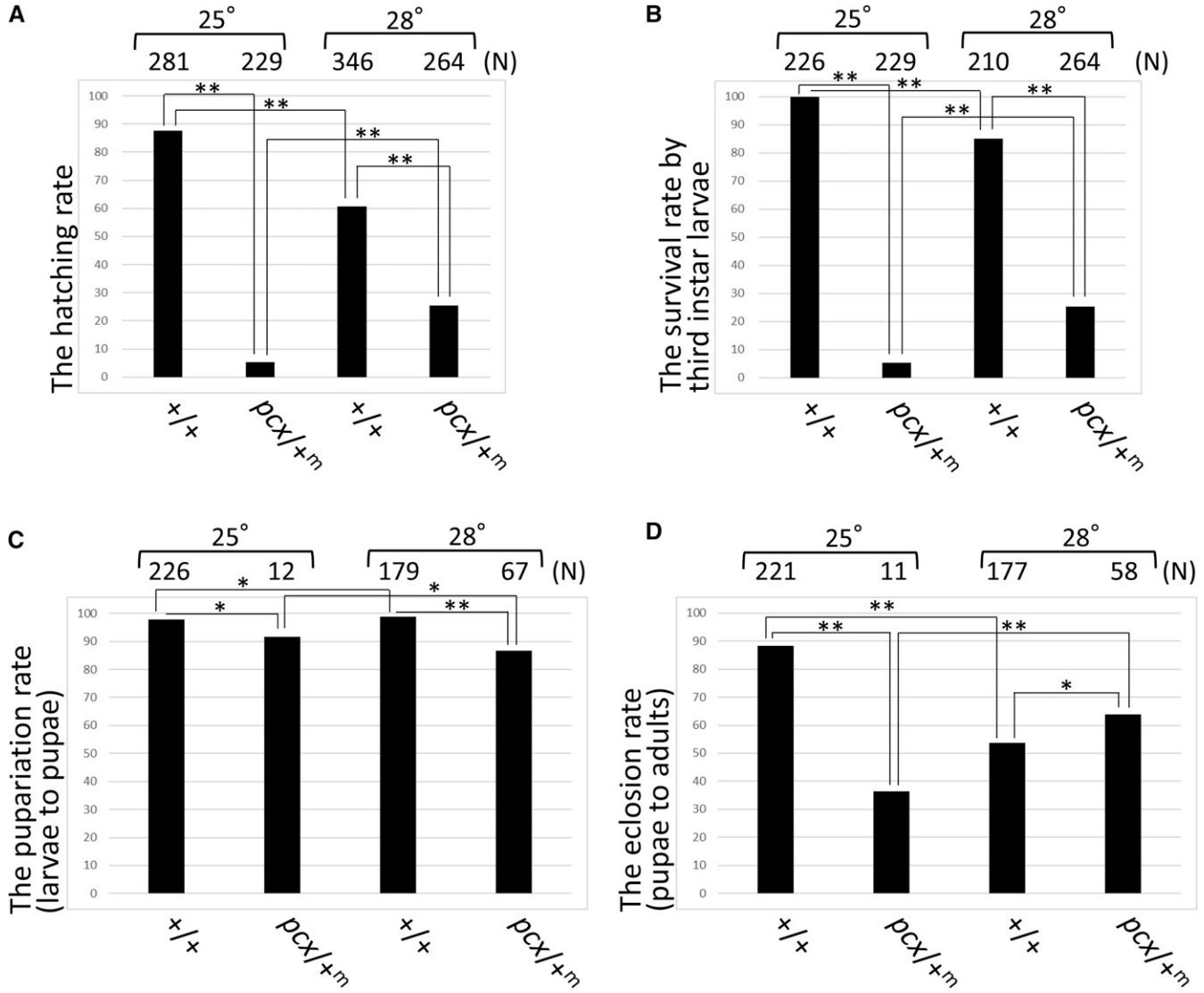

Figure 2 Survival rate of *pcx*/+^{m} is decreased at lower temperature. (A) Hatching rate of wild-type (+/+) and *pcx*/+^{m} females by the first-instar larval stage cultured at 25 or 28°. Percentages of total female embryos that became hatched female first-instar larvae are shown. For the calculation, half of the total embryos and hatched first-instar larvae were assumed to be female. The number of female embryos examined is shown as (N) at the top. (B) Survival rate of wild-type (+/+) and *pcx*/+^{m} females to the third-instar larval stage, cultured at 25 or 28°. Percentages of total female embryos that became surviving female third-instar larvae are shown. For the calculation, half of the total embryos were assumed to be female. The number of female embryos examined is shown as (N) at the top. (C) Pupation rate of wild-type (+/+) and *pcx*/+^{m} females cultured at 25 or 28°. The percentages of female third instar larvae that became pupae are shown. The number of female larvae examined is shown as (N) at the top. (D) Eclosion rate of wild type (+/+) females and *pcx*/+^{m} cultured at 25 or 28°. Percentages of pupae (sex was determined at the third-instar larval stage) that successfully eclosed as adults are shown. The number of female pupae examined is shown as (N) at the top. In (A and B), we rounded the deduced N down. All experiments were performed in triplicate. * $P > 0.01$, ** $P < 0.01$.

dominant suppressor; however, mutants affecting only the *BobA* locus were not available. Therefore, in this study, we generated a deletion mutant of *BobA*, *BobA*^{1}, as described below. For the *lov* gene, analyses using small Dfs defined the *lov* locus as a potential enhancer of *pcx*, and this possibility was confirmed using a preexisting *lov* mutant allele (Bjorum *et al.* 2013).

Mutagenesis of the BobA locus

A deletion mutant of *BobA* was generated using the FLP-FRT recombination method (Parks *et al.* 2004). Males carrying a *P*-element (PBac{RB}e00913) inserted in the 455-bp region upstream of *Twin of m4* (*Tom*) on the third chromosome were crossed with females carrying a FLP recombinase transgene (Thibault *et al.* 2004). Male progeny carrying both the *P*-element and FLP recombinase transgene were then mated with females carrying another *P*-element (PBac{WH}BobA^{f03024}) inserted in the 3′ untranslated region of the *BobA* gene (Thibault *et al.* 2004) (see Figure S7). After 2 days, the parents and progeny were transferred into a 37° water bath and incubated for 1 hr. The cultures were then incubated at 25°, and the parents were removed after 72 hr. Subsequently,

the progenies were subjected to heat-shock treatments at 37° for 1 hr once a day for 4 days. The virgin females of the progeny were then collected and mated with males containing a balancer, TM6B, which carries the *lacZ* gene, to establish stocks for further analysis.

Sequence analysis of the BobA[1] mutant allele

We established 14 potential lines of *BobA* mutants. Mutation of the *BobA* locus was confirmed by DNA sequence analysis. All polymerase chain reaction (PCR) assays were performed using purified genomic DNA from five embryos homozygous for each potential *BobA* mutant line. These homozygous embryos were selected based on the absence of X-gal staining (*lacZ*-negative) using a standard protocol (Ashburner 1989). Genomic DNA was extracted using a standard protocol (Parks *et al.* 2004). PCR primers flanking the two *P*-elements were designed (Forward primer 1, 5′-ACA GGG AGC ACA CAA TAA CGA TC-3′; Reverse primer 1, 5′-CAG AAG GGG TTT GAC CAG TTT C-3′). PCR was carried out using TaKaRa Prime Script GXL and a rapid protocol according to the manufacturer's instructions: 10 sec at 98°, 15 sec at 55°, and 20 sec at 68° (40 cycles). We isolated three lines that carried a deletion uncovering the *BobA* genomic region, based on the size of the PCR product. Unincorporated primers, nucleotides, and salts were removed using a Wizard SV Gel and PCR Clean-Up System (Promega). Then, 4 μl of each eluted PCR product was added to 1 μl of Big Dye Terminator v3.1 sequencing cocktail (Applied Biosystems) containing the following sequencing primers (Reverse primer 1 and Forward primer 2, 5′-ACA GAA AAC TGC CGA ACC AA-3′). After 25 cycles of PCR (10 sec at 96°, 5 sec at 50°, and 4 min at 60°), the products were separated using an Applied Biosystems 3130xl sequencer. The results revealed that we obtained a *BobA*[1] allele in which the entire *BobA* gene and a noncoding RNA gene, *CR45978*, were deleted.

Immunohistochemistry

Antibody staining of embryos was performed as previously described (Rhyu *et al.* 1994). The following primary antibodies were used: rat anti-Elav [7E8A10, 1:500; NIH Developmental Studies Hybridoma Bank (DSHB)], mouse anti-Sxl (M18, 1:10; DSHB), mouse anti-Dl (C594.9B, 1:500; DSHB), guinea pig anti-Dl (gp582, 1:100, a gift from S. Artavanis-Tsakonas), chicken anti-β-galactosidase (ab9361, 1:500; Abcam), rabbit anti-Rab11 (1:5000, a gift from A. Nakamura; Tanaka and Nakamura 2008), and rabbit anti-Rhomboid (1:500, a gift from E. Bier; Sturtevant *et al.* 1996) antibodies. The following secondary antibodies were used: Cy3-conjugated donkey anti-mouse (1:500; Jackson ImmunoResearch), Cy3-conjugated donkey anti-guinea pig (1:500; Jackson ImmunoResearch), Alexa488-conjugated donkey anti-rabbit (1:500; Jackson ImmunoResearch), Alexa488-conjugated donkey anti-rat (1:500; Jackson ImmunoResearch), Cy5-conjugated donkey anti-chick (1:500; Jackson ImmunoResearch), and Cy5-conjugated goat anti-mouse (1:500; Jackson ImmunoResearch) antibodies. Confocal microscopy images were captured using an LSM 700 (Zeiss) and analyzed on an LSM Image Browser, ZEN2010 (Zeiss).

Data availability

Strains are available upon request. File S1 contains all supplemental figures, tables and reagent table. Tables S1 and S2 contains lists of all *D. melanogaster* strains used for this screen. Supplemental material available at Figshare: https://doi.org/10.6084/m9.figshare.6395831

Results

pcx exhibits a cold-sensitive lethal phenotype

pcx is a maternal neurogenic gene, given that embryos homozygous or hemizygous for *pcx* without a maternal contribution of *pcx* (referred to as pcx^{mz} in this study), exhibit the neurogenic phenotype, which is a benchmark implicating a deficiency in Notch signaling (Perrimon *et al.* 1984; LaBonne *et al.* 1989). Furthermore, the maternal neurogenic phenotype can be paternally rescued, as the introduction of a paternal *pcx* locus into *pcx* heterozygotes lacking maternal *pcx* results in a much weaker neurogenic phenotype than that of pcx^{mz} (*pcx*/Y^{m} in males) at 25° (optimal conditions for *Drosophila*) (LaBonne *et al.* 1989; Yamakawa *et al.* 2012) (Figure 1A). Here, we refer to the heterozygote for *pcx* lacking maternal *pcx* (but containing paternal *pcx*) as "$pcx/+^{m}$." However, in a previous study, we discovered that $pcx/+^{m}$ is lethal at 25° in a standard *Drosophila* medium (Yamakawa *et al.* 2012). To analyze the lethality of $pcx/+^{m}$ further, in this study, we mated five *pcx* homozygous or wild-type virgin females with five wild-type males at 25°, and maintained the cultures at 25° (Figure 1A). Wild type showed normal development to pupae and adults at this temperature (Figure 1, B and C). However, only a small fraction of $pcx/+^{m}$ individuals reached the pupal stage, and none reached adulthood, under the same condition (Figure 1, B and C). Thus, the lethal phenotype associated with pcx^{mz} was not paternally rescued at 25°.

For some mutants of genes, including those encoding Notch-signaling components, the associated phenotypes are sensitive to a change in temperature (Leonardi *et al.* 2011; Shimizu *et al.* 2014; Ishio *et al.* 2015). The heat- or cold-sensitive properties of such mutations may be useful for performing genetic analyses, including genetic modifier screens, because the gene activity can be controlled by temperature shifts to reveal the phenotype (O'Connell *et al.* 1998; Dellinger *et al.* 2000; Lindsay *et al.* 2008). Thus, in the current study, we examined the lethal phenotypes of $pcx/+^{m}$ at different temperatures. As performed at 25°, we mated five *pcx* homozygous or wild-type virgin females with five wild-type males at 18 and 28° (Figure 1A). The cultures were maintained at each temperature, and the average number of female pupae and adults obtained from each culture vial was counted (Figure 1, B and C). We found that $pcx/+^{m}$ developed to pupae and adults at 28° but not at 18°, while wild type reached the adult stage at both temperatures (Figure 1,

B and C). In particular, the numbers of *pcx/+^{m}* pupae and adults increased markedly at 28°, compared with 25°. This difference was not attributed to temperature-dependent changes in the number of eggs laid by females of parental crosses at these two temperature, because we did not observe a marked difference in the numbers of eggs laid by wild-type and *pcx* homozygous females at 25° *vs.* 28° (Figure 1D). *pcx/Y^m* is reported to exhibit a neurogenic phenotype and embryonic lethality at 25° (Yamakawa, *et al.* 2012). However, because we did not determine the sex in Figure 1B it was possible that a portion of the *pcx/Y^m* embryos became viable at 28° until the pupal stage, to explain the increase in pupae observed. Therefore, to confirm that the *pcx/Y^m* embryos were embryonic lethal at 28°, we examined whether all of the male embryos cultured at this temperature showed a neurogenic phenotype. Male embryos (*pcx/Y^m*) were sorted out based on the absence of anti-Sexlethal (Sxl) antibody staining, and their neuronal cells were detected by anti-Elav antibody staining (Figure 1E) (Bopp *et al.* 1991). The repetitive structure of the ladder-like nervous system was observed in wild-type embryos (Figure 1E, +/Y), while the *pcx/Y^m* embryos exhibited a severe neurogenic phenotype in all cases examined at 28° (Figure 1E, *pcx/Y^m*). Thus, we concluded that *pcx/Y^m* males did not contribute to the observed change in the lethality, and that *pcx/+^{m}* exhibited a cold-sensitive lethal phenotype.

Given that *pcx/+^{m}* exhibited a clear cold-sensitive lethal phenotype, a change in the sex ratio could also have influenced the number of pupae and adults in our experiments. However, we found that the females of parental crosses laid almost the same percentage of female eggs (+/+ and *pcx/+^{m}*, respectively) at 25 and 28° (Figure 1G). In addition, the percentage of *pcx/+^{m}* females in the total embryos (*pcx/+^{m}* plus *pcx/Y^m*) laid by *pcx* homozygote mothers was almost the same at 25 and 28° (Figure 1G). Therefore, the sex ratio of the eggs laid by *pcx* homozygous females did not show a significant difference at these two temperatures. These results excluded the possibility that a change in the sex ratio contributed to the cold-sensitive lethality.

To determine the developmental stage responsible for the cold-sensitive lethality, we next compared the survival rate of *pcx/+^{m}* and wild type between these two temperatures at different developmental stages. First, we analyzed the hatching rates of wild-type and *pcx/+^{m}* embryos. To obtain the hatching rate, the number of female first-instar larvae (+/+ or *pcx/+^{m}*) was divided by the number of total female embryos, which was deduced by assuming that half of the total embryos were female. For the wild-type control, the number of female first-instar larvae was also deduced from the sex ratio. We found that the hatching rate of *pcx/+^{m}* was significantly increased at 28° compared with 25° (Figure 2A). In contrast, the hatching rate of wild type was slightly reduced at 28° compared with 25°, probably due to the nonoptimal temperature (Figure 2A). Therefore, we concluded that *pcx/+^{m}* shows cold-sensitive lethality during its embryonic stage. We also determined the rate of survival to the third-instar larval stage (Figure 2B). We calculated the percentage of deduced female wild-type and *pcx/+^{m}* embryos based on the sex ratio that reached the third-instar larval stage. The survival rate of *pcx/+^{m}* to the third-instar larval stage was significantly greater at 28° than at 25° (Figure 2B). Therefore, the cold-sensitive lethality of *pcx/+^{m}* could also be detected as the rate of survival to the third-instar larval stage, which was similar to the cold-sensitive hatching rate of the *pcx/+^{m}* embryos. Thus, the survival rate to the third-instar larval stage could be used to analyze the cold-sensitive lethality of *pcx/+^{m}* in combination with other mutants in the latter part of this study, which was useful because the sex and genotypes could be determined more easily at this stage, compared with those of first-instar larvae.

We also examined whether other developmental stages, such as pupation and eclosion, were involved in the cold-sensitivity of *pcx/+^{m}* lethality. To determine the pupation (percentage of third-instar larvae that became pupae) and eclosion (percentage of pupae that successfully eclosed) rates, we counted the female larvae at the third instar (*pcx/+^{m}* and +/+ in each experiment) based on gonad size and cultured them until pupation and eclosion. However, the pupation rates of *pcx/+^{m}* and wild-type females were not markedly different at 25° *vs.* 28° (Figure 2C). Therefore, once *pcx/+^{m}* embryos reached the third-instar larval stage, most of them developed to the pupal stage. We found that the eclosion rate of the *pcx/+^{m}* pupae was significantly greater at 28° than at 25° (Figure 2D). However, the eclosion rate of *pcx/+^{m} vs.* wild-type was not significantly different at 28°, probably because the eclosion rate of wild type was slightly lower at 28° than at 25° (Figure 2D). Thus, although the eclosion rate has some influence on the cold-sensitive lethality of *pcx/+^{m}*, it may not have a major effect. Collectively, these results showed that the cold-sensitive lethality of *pcx/+^{m}* was mostly associated with a reduction in the hatching rate.

The *pcx/+^{m}* that were cultured continuously at 28° reached adulthood, and these adult flies did not exhibit detectable defects in their overall morphology (data not shown). Thus, to detect the potential requirement of *pcx* during the pupal development, we also performed a stage-specific temperature-shift experiment from 28 to 25° during the larval and pupal stages. Such a temperature shift could cause some developmental defects in adulthood, because *pcx/+^{m}* individuals showed a slightly reduced eclosion rate at 25° compared to 28°, which suggested potential defects in their pupal development. We cultured *pcx/+^{m}* at 28° until the third-instar larval stage, then shifted the culture temperature to 18°. However, we did not observe a marked reduction in the number of eclosed flies under this temperature-shift condition (Figure 1C). Furthermore, the adult flies that experienced the temperature shift did not exhibit detectable defects, in particular those suggesting a reduction in Notch signaling, such as wing notch, wing-vein thickening, or rough eye (Figure 1F) (Shellenbarger and Mohler 1978; De Celis and García-Bellido 1994; Go *et al.* 1998). Thus, the cold-sensitive lethality of *pcx/+^{m}* did not appear to be directly attributable

to a decline in Notch signaling after the third-instar larval stage. This idea is consistent with our observation that the cold-sensitive lethality of *pcx*/+^{m} was mostly observed as a reduction in the hatching rate (Figure 2A).

The cold-sensitive phenotypes of pcx is due to a reduction in Notch signaling at lower temperatures

We next examined whether the cold-sensitive lethality of *pcx*/+^{m} was caused by a further reduction in Notch signaling at the lower temperature during embryogenesis. To test this possibility, we examined whether the cold-sensitive lethality of *pcx*/+^{m} embryos coincided with the extent of the neurogenic phenotype, detected by anti-Elav antibody staining, even though the neurogenic phenotype of *pcx*/+^{m} embryos was less prominent owing to paternal rescue (weak neurogenic phenotype), compared with that of *pcx*^{mz} embryos (strong neurogenic phenotype) at 25° (Figure 3, A–D) (Yamakawa *et al.* 2012). Wild-type embryos exhibited a normal central nervous system (CNS) and peripheral nervous system (PNS) at stage 14 (100%, $n = 47$) (Figure 3A). As previously reported, a strong neurogenic phenotype, characterized by neural hyperplasia of the CNS and PNS, was observed in the *pcx*^{mz} (*pcx*/*Y*^{m}) embryos, in which the zygotic and maternal *pcx* function was absent (100%, $n = 19$) at 25° (Figure 3B) (Yamakawa *et al.* 2012). We also observed the paternal rescue of the neurogenic phenotype in *pcx*/+^{m} embryos, in which the strong neurogenic phenotype was suppressed in all cases examined at 18° ($n = 47$), 20° ($n = 52$), 22° ($n = 102$), 25° ($n = 44$), 28° ($n = 51$), and 30° ($n = 34$), and the strong neurogenic phenotype was not observed at all (Figure 3, C–E). Among the paternally rescued embryos, we identified two classes of phenotypes in the embryonic nervous system: one exhibited a mostly normal nervous system as determined by its overview structure (quenched neurogenic phenotype) (Figure 3, C and E), whereas the other still showed a weak neurogenic phenotype, especially in the CNS, although the neural hyperplasia of the PNS was effectively suppressed (Figure 3, D and E). We observed that the percentage of embryos classified as weak neurogenic increased, and the percentage of quenched neurogenic embryos decreased, as the culture temperature was decreased (Figure 3E). The percentage of embryos classified as weak neurogenic was 80.9, 69.2, 68.6, 52.3, 31.4, and 14.7% at 18, 20, 22, 25, 28, and 30°, respectively (Figure 3E). These results suggested that the Notch signaling activity in *pcx*/+^{m} embryos decreased with the decline in temperature. Therefore, we concluded that the cold-sensitive lethality could be attributed, at least in part, to a reduction in Notch signaling in *pcx*/+^{m} embryos.

Genetic screens to identify mutations that dominantly modify the cold-sensitive phenotype of pcx

Using the cold-sensitive phenotype of *pcx*/+^{m}, we next conducted dominant modifier screens. First, we screened for dominant enhancers of the cold-sensitive lethality (Figure 4A). At 28°, *pcx*/+^{m} animals survived until adulthood, whereas this genotype was virtually lethal before adulthood at 25° (Figure 1, B and C). Therefore, we searched for second-site mutations that ameliorated the viability of *pcx*/+^{m} adults, thereby resulting in lethality prior to adulthood in a dominant manner at 28°. Second, we screened for dominant suppressors of the lethality that was observed in *pcx*/+^{m} at 25° (Figure 1B). In this screen, we looked for second-site mutations that resulted in the emergence of *pcx*/+^{m} adult flies at this temperature. In both screens, we used Df kits that carried chromosomal deletions of the second and third chromosomes on a uniform genetic background (see *Materials and Methods* and Figure 4A). We screened 189 and 179 deficiency lines on the second and third chromosomes, respectively (Table S1). These screens covered ~98% of the *Drosophila* genome (Cook *et al.* 2012).

Identification of dominant enhancers of pcx/+^{m}

In our dominant enhancer screen, we identified seven deficiencies that enhanced the cold-sensitive lethality of *pcx*/+^{m} in a dominant manner at 28° (Figure 4B). To identify the genetic loci responsible for the dominant enhancement, we narrowed down the genomic regions using smaller Dfs that uncovered smaller parts of the deleted regions in the seven positive Dfs identified in our first screen (Figure 4B and Figures S1–S6 and S8). *Df(2L)BSC50* and *Df(2L)BSC689* were positive Dfs carrying deletions that partially overlapped (Figure 4B and Figure S1). Among the smaller Dfs uncovering the genomic regions deleted in *Df(2L)BSC50* and *Df(2L)BSC689*, we found that *Df(2L)BSC205* and *Df(2L)BSC251*, but not other Dfs, enhanced the *pcx*/+^{m} lethality (Figure 4B and Figure S1). The genomic deletions in *Df(2L)BSC205* and *Df(2L)BSC251* partially overlapped, and the *bib* locus exists in the overlapping region (Figure S1). *bib* is a classic neurogenic gene that encodes a component of the Notch signaling pathway (Lehmann *et al.* 1983; Doherty *et al.* 1997). The deduced product of *bib* has high homology to mammalian aquaporin-4, although a water channel activity of Bib was not detected in previous studies (Kaufmann *et al.* 2005; Park *et al.* 2008). In the current study, we found that *bib*^{1}, an existing allele of *bib*, dominantly enhanced the cold-sensitive lethality of *pcx*/+^{m} (Figure 5A, *pcx*/+^{m}; *bib*^{1}/+). However, the heterozygote for *bib*^{1} showed normal development to adulthood at 28°, demonstrating a synergistic interaction between *pcx* and *bib* (Figure 5A, +/+; *bib*^{1}/+). From these results, *bib* was identified as a dominant enhancer of *pcx*.

Using the same approach, we identified the genetic loci that were uncovered in each positive deficiency and responsible for dominant enhancement of the cold-sensitive lethality of *pcx*/+^{m} (Figures S2–S6 and S8). Among the small deficiencies overlapping *Df(3R)ED5938*, we found that *Df(3R)BSC850* and *Df(3R)ED5942*, which partially overlapped each other, enhanced the lethality of *pcx*/+^{m} (Figure 4B and Figure S2). Notably, the overlapping region contained the *Dl* locus (Figure S2). *Dl* encodes a ligand for the Notch receptor (Vässin *et al.* 1987; Kopczynski *et al.* 1988). We found that *Dl*^{5F102}, a preexisting allele of *Dl*, dominantly enhanced the lethality of *pcx*/+^{m} (Figure 4B

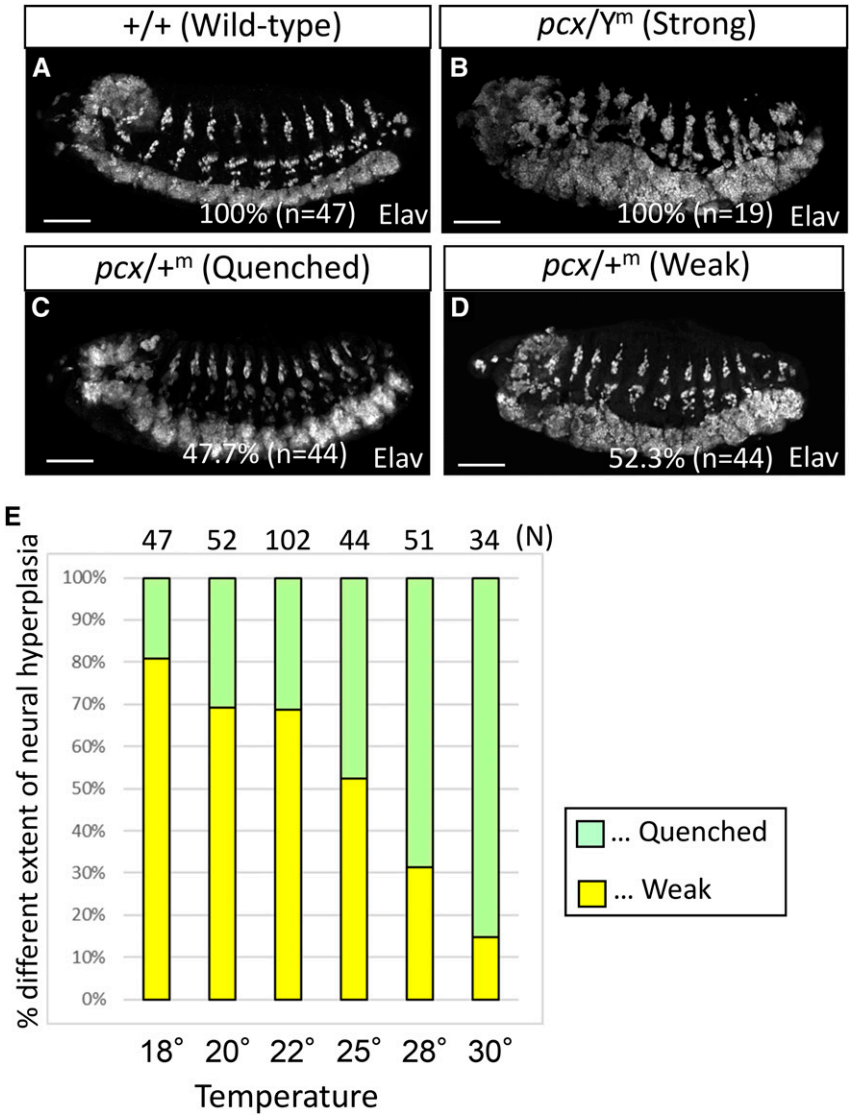

Figure 3 *pcx*/+^{m} exhibits a cold-sensitive neurogenic phenotype. (A–D) Lateral views of embryos cultured at 25° and immunostained with a neuron-specific antibody (anti-Elav antibody) at stage 13–14. (A) Wild type (+/+). (B) *pcx*^{mz} (*pcx*/*Y*^{m}) embryo showing a strong neurogenic phenotype (100%, *n* = 19) ("Strong"). (C) *pcx*/+^{m} embryo showing a mostly normal nervous system structure (quenched neurogenic phenotype) (47.7%, *n* = 44) ("Quenched"). (D) *pcx*/+^{m} embryo showing a weak neurogenic phenotype (52.3%, *n* = 44) ("Weak"). In (A–D), Bar, 50 μm. (E) Percentage of *pcx*/+^{m} embryos showing a mostly normal nervous system (quenched, green) and a weak neurogenic phenotype (weak, yellow) at the indicated temperatures. Number of embryos examined in each experiment (N) is indicated at the top.

and Figure 5A, *pcx*/+^{m}; *Dl*^{5F102}/+). In contrast, heterozygotes for *Dl*^{5F102} developed normally to adulthood at 28° (Figure 5A, +/+; *Dl*^{5F102}/+). Thus, we identified *Dl* as another dominant enhancer of *pcx*. Another of the seven deficiency lines identified by our screens was *Df(3R) ED5330*, which contained the *neur* locus within its deleted genomic region (Figure 4B and Figure S3). We found that *neur*^{1}, a preexisting allele of *neur*, dominantly enhanced the lethality of *pcx*/+^{m} (*pcx*/+^{m}; *neur*^{1}/+), although *neur*^{1}/+ flies developed normally to adulthood at 28° (Figure 4B and Figure 5A). Thus, *neur* was also identified as a dominant enhancer of *pcx*. Thus, our enhancer screen of the cold-sensitive lethality of *pcx*/+^{m} at 28° identified three genes, *bib*, *Dl*, and *neur*, all of which encode known components of the Notch signaling pathway, as dominant enhancers of *pcx*.

On the other hand, in the genomic regions deleted in *Df(2R)Kr10*, which was also identified as dominant enhancer of *pcx*, we failed to find a gene that was known to be involved in Notch signaling (Figure 4B and Figure S4). However, it was possible that gene(s) encoding novel component(s) of the Notch signaling pathway exist in these regions, given that three genes involved in Notch signaling were successfully identified by our enhancer screen as described above. Therefore, using small Dfs, we attempted to narrow down the genomic region containing the dominant enhancer to single loci. The genomic deletion in *Df(2R)Kr10* partially overlapped with two small Dfs, *Df(2R)GGG*^{d13} and *Df(2R)gsb* (Figure 4B and Figure S4). We found that *Df(2R)gsb*, which overlapped with the *lov* locus, enhanced the cold-sensitive lethality of *pcx*/+^{m} at 28°, but *Df(2R)GGG*^{d13}, which did not overlap with the *lov* locus, did not (Figure S4). These results collectively suggested that *lov* may be responsible for the dominant enhancement of lethality (Figure S4). We found that an available *lov* allele, *lov*^{47}, dominantly enhanced the lethality of *pcx*/+^{m} at 28° (Figure 5B, *pcx*/+^{m}; *lov*^{47}/+). However, *lov*^{47}/+ flies developed normally to adulthood at 28° (Figure 5B, +/+; *lov*^{47}/+). Thus, we concluded that *lov* is also a dominant enhancer of *pcx*, and demonstrated for the

A

♀♀ $\frac{pcx}{pcx}$ X ♂♂ $\frac{+}{Y}$; $\frac{\text{Deficiency (Df)}}{\text{Balancers (2nd or 3rd)}}$

↓

All females without balancers are zygotic *pcx* heterozygous flies lacking its maternal contribution and one copy of Df (*pcx*/+^{m}; Df/+).

↓

Viable Df are screened at 25°
Lethal Df are screened at 28°

B

28° lethal (Enhancer)

Df		Small Df		Tested allele		
Symbol No.	Deleted region	Symbol No.	Deleted region	Allele name	Molecular function	Cellular processes
Df(2L)BSC50	30F4-31B1	Df(2L)BSC205	30F5-31A2	*bib*^{1},	Aquaporin	Notch signaling
Df(2L)BSC689	30F5-31B1	Df(2L)BSC251	30F5-31A1			
Df(3R)ED5938	91D4-92A11	Df(3R)BSC850	91F11-92A6	*Dl*^{5F102}	Notch ligand	Notch signaling
		Df(3R)ED5942	91F12-92B3			
Df(2R)X58-12	58D1-59A	—	—	—	—	—
Df(2R)X58-8	58B3-59A1					
Df(2R)Kr10	60E10-60F5	Df(2R)gsb	60E12-60F4	*lov*^{47}	DNA binding	Gravitaxis
Df(3R)ED5330	85A5-85D1	—	—	*neur*^{1}	E3 ubiquitin ligase	Notch signaling

25° viable (Suppressor)

Df		Small Df		Tested allele		
Symbol No.	Deleted region	Symbol No.	Deleted region	Allele name	Molecular function	Cellular processes
Df(3L)ED217	70F4-71E1	Df(3L)BSC441	71A1-71B4	*BobA*^{1}	Bearded family	Notch signaling
Df(3R)ED5622	87F10-88A4	—	—	*Nsf2*^{A6}, *Nsf2*^{A15} *Nsf2*$^{urd-2}$	ATPase	SNARE-complex disassembly

Figure 4 Genetic screen procedure and summary of the dominant modifiers of *pcx*. (A) Five *pcx* homozygous females were mated with five males of each Deficiency (Df) mutant on the second or third chromosome at 25 or 28°. The genotype of F1 females without balancers was identified as *pcx*/+^{m}; Df/+. After 18 days, the numbers of F1 progeny were counted. *pcx*/+^{m} individuals survived until adulthood at 28°. In the enhancer screen, the Df lines that showed reduced viability at 28° (*i.e.*, those in which F1 did not survive until adulthood) were identified. *pcx*/+^{m} individuals were lethal by the pupal stage at 25°. In the suppressor screen, Df lines that suppressed the lethality at 25° (*i.e.*, those in which F1 survived to adulthood) were identified. (B) Tables summarizing the dominant enhancers [28° lethal (Enhancer)] and suppressors [25° viable (Suppressor)] of *pcx*/+^{m}. Df lines (Symbol No.) identified as dominant modifiers of *pcx*/+^{m} in the first screens and the deleted genomic region (Deleted region) in each Df line are listed in the left columns (Df). The small Df lines (Symbol No.) uncovering smaller parts of the original Dfs and containing the potential loci of the modifiers are listed in the middle columns (Small Df) with the deleted genomic regions (Deleted region). Dominant modifiers identified as single genes are indicated in the right columns (Tested allele) with information about the alleles (Allele name), molecular functions of the gene products (Molecular function), and potential associated cellular processes (Cellular process). "–" indicates inapplicable.

first time that *lov* may be involved in the Notch signaling pathway. Finally, we also identified two partially overlapping Dfs, *Df(2R)X58-12* and *Df(2R)X58-8*, from the dominant enhancer screen (Figure 4B and Figure S5). In this case, we failed to identify a preexisting mutation(s) that enhanced the lethality of *pcx*/+^{m} in the overlapping region of these two Dfs, although we excluded *CG3927*, *Vacuolar protein sorting 20* (*Vps20*), *bonsai*, and *Ribosomal protein 624* (*Rp624*) from the candidates for the modifier gene (Figure S5). Therefore, these Dfs were not analyzed further in this study.

We found that the cold-sensitive lethality of *pcx*/+^{m} could be easily assessed as a reduction in the rate of survival to the third-instar larval stage (Figure 2B). Thus, we evaluated the effect of these dominant enhancers on the viability of *pcx*/+^{m} based on the survival rate at this stage. We found that all four enhancers, *bib*, *Dl*, *neur*, and *lov*, significantly reduced the survival rates in a dominant manner, when each was combined with *pcx*/+^{m} at 28° (Figure 5, D and E). However, *bib*^{1}/+ and *neur*^{1}/+ did not show significantly different survival rates from wild type at 28° (Figure 5D). In contrast, the survival rates of *Dl*^{5F102}/+ and *lov*^{47}/+ were reduced to about half that of wild type (Figure 5, D and E). However, the survival rates observed in these heterozygous embryos were not as low as those of embryos with these enhancers combined with *pcx*/+^{m} (Figure 5, D and E). Therefore, we concluded that *bib*, *Dl*, *neur*, and *lov* dominantly enhanced the lethality of *pcx*/+^{m} from the third-instar larval stage to the embryonic stage.

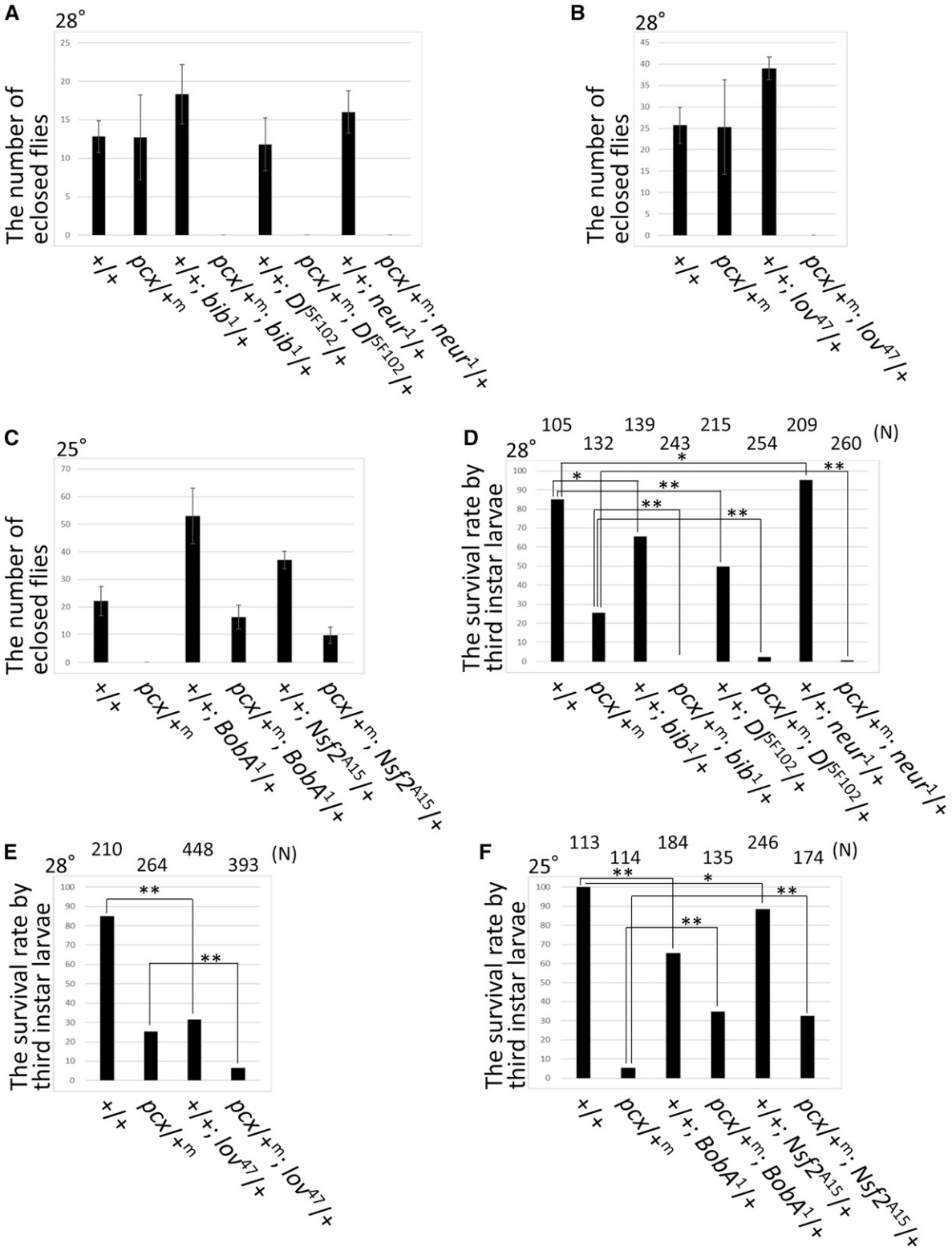

Figure 5 Dominant modification of the cold-sensitive lethality of *pcx*/+^{m} by *pcx* modifiers identified as single loci. (A) The numbers of female adult flies of wild type (+/+), *pcx*/+^{m}, heterozygotes of each enhancer (*bib*^{1}, *Df*^{5F102}, or *neur*^{1}), and *pcx*/+^{m} combined with *bib*^{1}/+, *Df*^{5F102}/+, or *neur*^{1}/+ at 28° are shown. Genotypes were determined by sex and marker phenotypes associated with balancer chromosomes. (B) Numbers of female adult flies of wild type (+/+), *pcx*/+^{m}, heterozygote of *lov*^{47}, and *pcx*/+^{m} combined with *lov*^{47}/+ at 28° are shown. Genotypes were determined by sex and marker phenotypes associated with balancer chromosomes. (C) Numbers of female adult flies of wild type (+/+), *pcx*/+^{m}, heterozygotes of each suppressor (*BobA*^{1} and *Nsf2*^{A15}), or *pcx*/+^{m} combined with *BobA*^{1}/+ and *Nsf2*^{A15}/+ at 25°. Genotypes were determined by sex and marker phenotypes associated with balancer chromosomes. (D) Survival rate of wild-type (+/+) females, *pcx*/+^{m}, and heterozygous females of each enhancer (*bib*^{1}, *Df*^{5F102}, or *neur*^{1}),

Identification of dominant suppressors of pcx/+^{m}

At 25°, *pcx*/+^{m} failed to develop to adulthood. We next screened for Dfs that suppressed the cold-sensitive lethality of *pcx*/+^{m} in a dominant manner at 25° (Figure 4A and Table S1), and identified *Df(3L)ED217*. The genomic region deleted in *Df(3L)ED217* was partially uncovered in six small deficiencies, *Df(3L)BSC441*, *Df(3L)Exe16125*, *Df(3L)Exe16126*, *Df(3L)BSC837*, *Df(3L)ED218*, and *Df(3L)Exe16262* (Figure 4B and Figure S6). We found that among these six small Dfs, only *Df(3L)BSC441* dominantly suppressed the lethality of *pcx*/+^{m} at 25° (Figure 4B and Figure S6). Five genes, *CG17839*, *CG34245*, *DCX-EMAP*, *CG13465*, and *BobA* existed in the genomic region encompassed by *Df(3L)BSC441*, which contained the locus responsible for the dominant suppression. Among these, *DCX-EMAP* was the only gene with an available mutant (Bechstedt *et al.* 2010). However, *DCX-EMAP* did not suppress the lethality, which excluded this gene as the dominant suppressor. To identify the dominant suppressor as a single locus, we next generated a *BobA* mutant allele, because *BobA* is a member of the *Bearded* (*Brd*) family, which is known to negatively regulate Notch signaling (Lai *et al.* 2000). Brd family members bind to and inhibit Neur, an E3 ubiquitin ligase that ubiquitinates Dl (Bardin and Schweisguth 2006). The ubiquitination of Dl is required for endocytosis of Dl, which facilitates the signaling activity of Dl (Lai *et al.* 2001; Le Borgne *et al.* 2005). However, the specific functions of *BobA* have remained unknown, because a mutation affecting only the *BobA* locus has not been available. In addition, the previous study was based on deletion mutants uncovering multiple *Brd* family genes, including *BobA* (Bardin and Schweisguth 2006). Thus, in the current study, we generated a mutant allele of *BobA*, designated as *BobA*^{1}, using the FLP-FRT recombination method (Figure S7). Thus, *BobA^1* is the first mutant in which a single *Brd* family gene was disrupted. We found that *BobA*^{1} dominantly suppressed the lethality of *pcx*/+^{m} at 25° (Figure 4B and Figure 5C, *pcx*/+^{m}; *BobA^1*/+). In addition, a gene encoding a noncoding RNA, *CR45978*, was also deleted in *BobA*^{1} (see Figure S7) (Young *et al.* 2012). However, it is unlikely that *CR45978* is the dominant suppressor of *pcx*/+^{m} lethality, because *CR45978* expression has only been detected in adult males (Young *et al.* 2012). Thus, our results suggested that *BobA* is a dominant suppressor of *pcx*.

Notably, the Df kits used in our screens have small gaps in the coverage of deleted genomic regions, corresponding to ~2% of the chromosomes (Cook *et al.* 2012). Thus, the genes located within these gaps had escaped from our screens. To minimize this occurrence, we examined an additional 30 preexisting small Dfs that uncovered the gap regions on the second and third chromosomes (Table S2). Among these, *Df(3R)ED5662* dominantly suppressed the cold-sensitive lethality of *pcx*/+^{m} at 25° (Figure 4B and Table S2). We found that this Df uncovered the *N-ethylmaleimide-sensitive factor 2* (*Nsf2*) gene, which was previously identified as a modifier of Notch signaling (Figure S8) (Stewart *et al.* 2001). We here showed that a preexisting allele of *Nsf2*, *Nsf2^{A15}* dominantly suppressed the cold-sensitive lethality of *pcx*/+^{m} at 25° (Figure 4B and Figure 5C, *pcx*/+^{m}; *Nsf2^{A15}*/+). This result identified *Nsf2* as a dominant suppressor of *pcx*.

Based on the above findings, we speculated that the dominant suppression of the cold-sensitive lethality of *pcx*/+^{m} might be due to an increase in the survival rate to the third-instar larval stage. We found that *BobA^1* and *Nsf2^{A15}* significantly increased this survival rate in a dominant manner when combined with *pcx*/+^{m} at 25° (Figure 5F, *pcx*/+^{m}; *BobA^1*/+ and *pcx*/+^{m}; *Nsf2^{A15}*/+, respectively). *BobA^1*/+ by itself showed a slightly decreased survival rate (Figure 5F, +/+; *BobA^1*/+). However, we might be able to ignore this effect, because the number of eclosed *BobA^1*/+ flies was comparable to that of wild type at 25° (Figure 5C). These results suggested that *BobA^1* and *Nsf2^{A15}* dominantly suppressed the lethality of *pcx*/+^{m} from the embryonic to the third-instar larval stage.

pcx modifiers influence Notch signaling activity

Our genetic screens identified four dominant enhancers and two dominant suppressors of the cold-sensitive lethality of *pcx*/+^{m}. As described above, in *pcx*/+^{m}, we observed a correlation between the extent of cold-sensitive lethality and the neurogenic phenotype, which is an indicator of reduced Notch signaling activity (Simpson 1990). In addition, we found that the dominant enhancers and suppressors reduced and increased the survival rate by the third-instar larval stage, respectively, suggesting that these modifiers affect embryonic development, such as the neuroblast segregation controlled by Notch signaling. Therefore, we next examined whether these enhancers and suppressors also modified the neurogenic phenotype of *pcx*/+^{m}. At 28°, 31.4% of the *pcx*/+^{m} embryos showed a weak neurogenic phenotype, whereas the rest of the embryos exhibited a largely normal nervous system (quenched neurogenic phenotype), based on

and *pcx*/+^{m} combined with *bib^1*/+, *Dl^{5F102}*/+, or *neur^1*/+ to the third-instar larval stage at 28°. Percentages of surviving female third-instar larvae with the indicated genotype in the deduced total number of female embryos with that genotype are shown. (E) Survival rate of wild-type (+/+) females, *pcx*/+^{m}, heterozygous females of *lov^{47}*, and *pcx*/+^{m} combined with *lov^{47}*/+, to the third-instar larval stage at 28°. Percentages of surviving female third-instar larvae with the indicated genotype in the deduced total number of female embryos with that genotype are shown. (F) Survival rate of wild-type (+/+) females, *pcx*/+^{m}, heterozygous females of each suppressor (*BobA^1* and *Nsf2^{A15}*), or *pcx*/+^{m} combined with *BobA^1*/+ and *Nsf2^{A15}*/+, to the third-instar larval stage at 25°. Percentages of surviving female third-instar larvae with the indicated genotype in the deduced total number of female embryos with that genotype are shown. In (D–F), genotypes were determined by sex and marker phenotypes associated with balancer chromosomes at the third-instar larval stage. In (D–F), for the calculation, the numbers of embryos with the indicated genotypes were predicted based on Mendel's laws, and half of the embryos were assumed to be female. In (D–F), the number of female embryos examined is shown as (N) at the top of each graph. We rounded the deduced N down. All experiments were performed in triplicate. In (A–C), SD are indicated. In (D–F), * $P > 0.01$, ** $P < 0.01$.

the criteria described in Figure 3. However, in combination with *pcx*/+^{m}, all of the dominant enhancers identified by our screen; *i.e.*, *bib*, *neur*, *Dl*, and *lov*, increased the percentage of embryos showing a weak neurogenic phenotype to 75.9, 78.5, 81.8, and 76.3%, respectively, in a dominant manner at 28° (Figure 6A). We also found that *bib*^{1}/+, *Dl*^{5F102}/+, *neur*^{1}/+, and *lov*^{47}/+ exhibited a normal nervous system (normal) upon anti-Elav antibody staining at 28°, suggesting that a synergistic genetic interaction, rather than a simple additive effect, occurred between *pcx* and each mutant (Figure 6A). Under the same conditions, an arbitrarily selected deficiency, *Df*(*2R*)*DE2457*, did not markedly affect the frequency of the *pcx*/+^{m} phenotypes (Figure 6A). These results suggested that the identified dominant enhancers further reduced the Notch signaling in *pcx*/+^{m} embryos.

We next examined whether the dominant suppressors identified by our screen suppressed the neurogenic phenotype of *pcx*/+^{m}. At 25°, 46.7% of the *pcx*/+^{m} embryos showed a weak neurogenic phenotype, while the rest showed a quenched neurogenic phenotype (n = 15) (Figure 6B). However, the two dominant suppressors, *BobA*^{1} (6.1%, n = 33) and *Nsf2*^{A15} (0%, n = 21), almost completely suppressed the neurogenic phenotype of *pcx*/+^{m} in a dominant manner at 25°, at which almost all of these embryos exhibited a quenched neurogenic phenotype (Figure 6B). Conversely, under the same conditions, an arbitrarily selected deficiency, *Df*(*2R*)*DE2457*, did not markedly affect the frequency of the weak neurogenic phenotype (64.7%, n = 34) (Figure 6B). These results suggested that mutations of the *BobA* and *Nsf2* genes augmented the Notch signaling activity in *pcx*/+^{m} embryos. We also found that *BobA*^{1}/+ and *Nsf2*^{A15}/+ exhibited a normal nervous system (normal) upon anti-Elav antibody staining at 25°, demonstrating that *BobA*^{1} and *Nsf2*^{A15} showed a synergistic genetic interaction with *pcx* (Figure 6B).

BobA may have a similar function as other Brd family genes in neuroblast segregation as well as in mesoderm specification

The endocytosis of Dl shows dorsal-ventral polarity in the cellular blastoderm at stage 5 (Bardin and Schweisguth 2006). Dl endocytosis is active in the ventral part (mesoderm) of embryos, depends on Neur, and is required for the spatially controlled activation of Notch signaling in the mesectoderm (Bardin and Schweisguth 2006). It was previously shown that *neur* activity is suppressed in the dorsal region of embryos by *Brd* family genes, so Dl trafficking is upregulated in this region in mutants of *Brd* family genes (Bardin and Schweisguth 2006; De Renzis *et al.* 2006). Thus, the Brd family proteins suppress Neur activity, leading to reduced Dl trafficking in the early embryo. In these experiments, however, multiple *Brd* family genes were simultaneously removed by a deletion mutation. In the current study, we found that the *BobA*^{1} mutant, in which only the *BobA* gene was deleted among the *Brd* family genes, suppressed the neurogenic phenotype (6.1%, n = 33) associated with *pcx*/+^{m}, compared with the wild-type *BobA* gene (46.7%, n = 15) (Figure 6B). In addition, although the role of the Dl-Neur-Brd pathway in specification of the mesectoderm has been extensively analyzed (Bardin and Schweisguth 2006), and it was proposed that the inhibition of Neur by Brd regulates the epithelial polarity (Chanet and Schweisguth 2012), its role in neuroblast segregation in the neuroectoderm has not been studied. Therefore, in this study, it was important to determine whether Dl trafficking was also upregulated in the *BobA*^{1} mutant embryos, especially in the neuroectoderm.

The distribution of Dl was analyzed by anti-Dl antibody staining. As previously shown, Dl was detected in recycling endosomes, which were specifically labeled by anti-Rab11 antibody staining, in the ventral but not the dorsal side of wild-type embryos at stage 5 in all cases examined (n = 5) (Figure 7) (Wang and Struhl 2004; Emery *et al.* 2005). However, Dl was ectopically detected in Rab11-positive vesicles in the dorsal side of *BobA*^{1} homozygous embryos at stage 5 in all cases examined (n = 8) (Figure 7). This observation was consistent with a previous finding that *Brd* family genes suppress the *neur*-dependent endocytosis of Dl in the dorsal but not the ventral side (Bardin and Schweisguth 2006). Importantly, we detected the Dl-containing ectopic vesicles in the neuroectoderm of *BobA*^{1} mutant embryos (n = 7), which was visualized by specific staining with an anti-Rhomboid antibody (left side of each panel in Figure 8; boundaries of Rhomboid-expressing and nonexpressing regions are indicated by a white broken line) (Sturtevant *et al.* 1996). In addition, notably, we found that *BobA*^{1} homozygous embryos showed an anti-neurogenic phenotype at 41.2% (n = 17) frequency at 28°, as revealed by a reduction in neuronal cells detected by anti-Elav antibody staining, whereas wild-type embryos did not show this phenotype at this temperature in any case examined (n = 27). Thus, our results suggest that the Dl-Neur-Brd pathway also regulates Dl endocytosis in the neuroectoderm during neuroblast segregation. On the other hand, we did not detect a notable difference in the number of Dl-containing vesicles in the ventral region of these embryos (Figure 7 and right sided of each panel in Figure 8), probably because the *Brd* genes are not expressed in the ventral region of wild-type embryos (Chanet and Schweisguth 2012).

Based on these results, BobA appears to have a similar activity to that of other Brd family proteins. This idea is consistent with the previous finding that the majority of Brd family proteins, including BobA, bind to Neur (Bardin and Schweisguth 2006). Conversely, our results also showed that the function of Brd family genes is not completely redundant regarding the suppression of Dl endocytosis and the ectopic activation of Notch signaling in the neuroectoderm. We predicted that if *pcx* is also directly involved in the Neur-mediated endocytosis of Dl, the number of Dl-positive vesicles should decrease in the mesoderm of *pcx*^{mz} embryos, as previously found in embryos homozygous for *neur* or overexpressing a Brd family gene (Bardin and Schweisguth 2006). However, we did not observe any abnormality in Dl-positive vesicles in the *pcx*^{mz} embryos in any case examined (n = 5) (Figure 7). We also examined whether there was a synergistic effect between *pcx* and *BobA* on the Dl

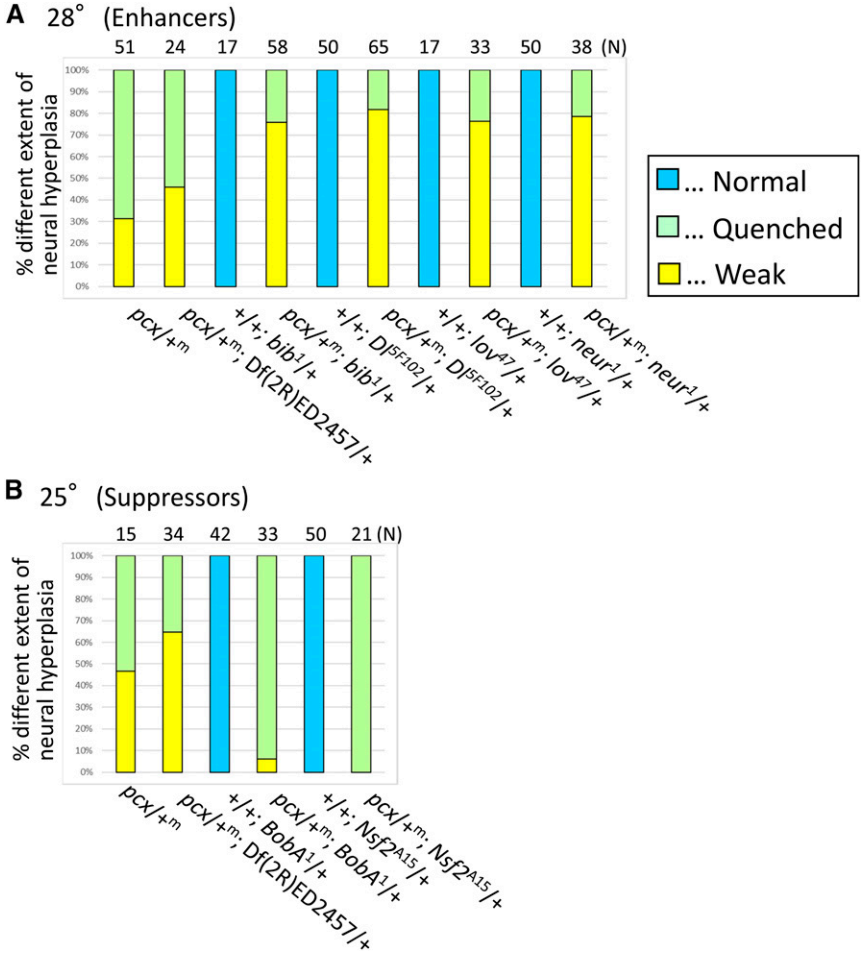

Figure 6 Dominant modification of the neurogenic phenotype of *pcx*/+^{m} by *pcx* modifiers. (A) Percentages of embryos showing a normal nervous system (normal, blue bars), quenched neurogenic phenotype (quenched, green bars), and weak neurogenic phenotype (weak, yellow bars) at 28°. Embryos of *pcx*/+^{m}, *pcx*/+^{m} combined with *Df(2R)ED2475*/+ (an arbitrarily selected deletion as a control), *bib*^{1}/+, *Dl*^{5F102}/+, *lov*^{47}/+, or *neur*^{1}/+, and heterozygotes of each enhancer (*bib*^{1}/+, *Dl*^{5F102}/+, *lov*^{47}/+, or *neur*^{1}/+) were analyzed. Embryos heterozygous for all the enhancers were scored as normal; none of them showed a dominant neurogenic phenotype at 28°. (B) Percentages of embryos showing normal nervous system (normal, blue bars), quenched neurogenic phenotype (quenched, green bars), and weak neurogenic phenotype (weak, yellow bars) at 25°. Embryos of *pcx*/+^{m}, *pcx*/+^{m} combined with *Df(2R)ED2475*/+ (an arbitrarily selected deletion as a control), *BobA*^{1}/+, or *Nsf2*^{A15}/+, and heterozygotes of each suppressor (*BobA*^{1}/+ or *Nsf2*^{A15}/+) were analyzed. Embryos heterozygous for each suppressor were scored as normal; none of them showed a dominant neurogenic or anti-neurogenic phenotype at 25°. The number of embryos examined in each experiment (N) is indicated at the top of the graph.

trafficking by combining *pcx*/+^{m} and *BobA*/+, in each of which the Dl-containing vesicles did not show any detectable abnormality. However, we did not observe any alteration in the Dl-positive vesicles in *pcx*/+^{m}; *BobA*/+ (Figure 9). Therefore, at this point, the molecular mechanisms underlying the genetic connection between the Dl-Neur-Brd pathway and Pcx remain unknown.

Discussion

Genes encoding known and novel components of Notch signaling were identified as dominant modifiers of pcx

Our dominant modifier screens of *pcx* identified four enhancers and two suppressors (Figure 4B). Among these, four genes encode well-characterized components of the Notch signaling pathway, suggesting that our procedure efficiently screened for Notch-signaling components. Although our primary screens were based on the enhancement and suppression of the cold-sensitive lethality demonstrated in *pcx*/+^{m} embryos, such modifications of this lethality coincided well with the enhancement and suppression of the neurogenic phenotype, implying that the lethality is related to a depletion of Notch signaling. Thus, the primary cause of the cold-sensitive lethality was probably a further reduction of Notch signaling with the decrease in temperature, and the modifications of the lethal phenotype reflected up- or down-regulations of Notch signaling in the heterozygous combination with each modifier.

We predicted that the phenotypes of *pcx*/+^{m} could have resulted from an alteration in the initial timing of the zygotic expression of *pcx*. However, in our screen, mutations that might have generally changed the onset of zygotic gene expression in the early embryo, such as chromatin remodeling factors, were not identified. Conversely, most of the identified genes were found to encode factors that directly contribute to the Notch signaling cascade. The highly specific genetic interactions between *pcx* and these genes support the idea that Pcx is a critical component of Notch signaling, at least during the period of neuroblast segregation in the neuroectoderm. This idea is also consistent with our previous finding that the expression of Notch signaling target genes, including *Enhancer of split* and *single-minded*, is severely reduced in *pcx*^{mz} embryos (Yamakawa *et al.* 2012).

The Dl-Neur-BobA pathway functions not only in mesectoderm specification but also in neuroblast segregation

Our screens identified the *Dl*, *neur*, and *BobA* genes, which have been shown to function in a common biochemical

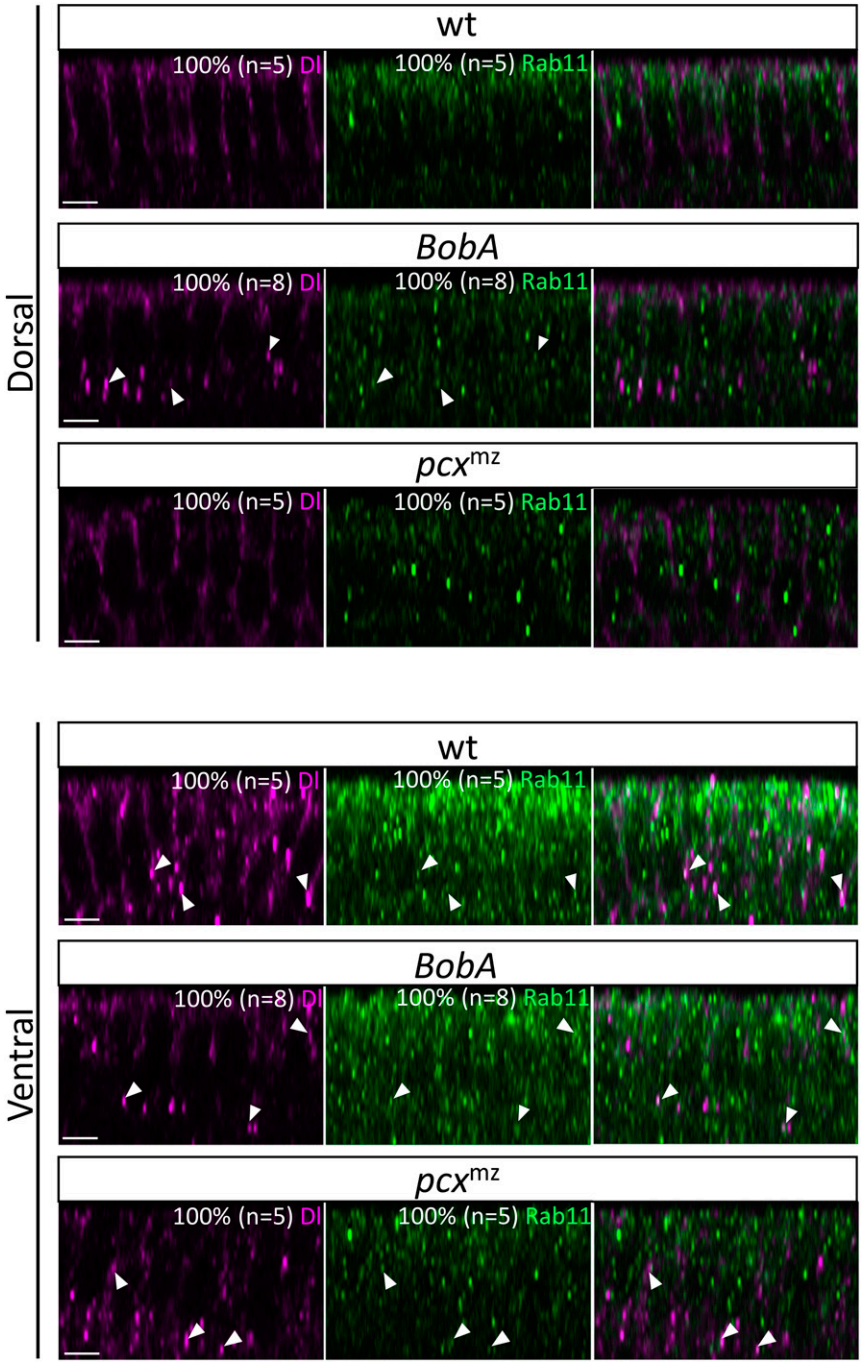

Figure 7 *BobA* suppresses Dl endocytosis in the dorsal region of embryos. Subcellular localization of Dl (magenta, left, and right panels) and Rab11 (green, middle, and right panels), a marker of recycling endosomes, in the dorsal (upper panels) and ventral (lower panels) epithelium of wild-type (wt), $BobA^{1}/BobA^{1}$ (*BobA*), and pcx^{mz} embryos at stage 5. Right panels are merged images of the left and middle panels. White arrowheads indicate vesicles where Dl and Rab11 are colocalized. Percentage of embryos showing the represented phenotypes is indicated at the upper right. The number of embryos examined is in parentheses. Bar, 5 μm.

process that regulates the dorsal-ventral pattern of Dl endocytosis, as dominant modifiers of *pcx* (Bardin and Schweisguth 2006; De Renzis *et al.* 2006). The activity of Dl as a ligand for Notch requires the endocytosis of Dl, which depends on the ubiquitination of the cytoplasmic domain of Dl by Neur, a RING domain-containing E3 ubiquitin ligase (Lai *et al.* 2001; Pavlopoulos *et al.* 2001). During early embryogenesis around stage 5, the endocytosis of Dl is particularly active in the mesoderm located in the most ventral part of the embryo, although Dl endocytosis is much less active in the neuroectoderm that is dorsally adjacent to the mesoderm. Therefore, the high Dl activity in the mesoderm induces the Notch signaling-dependent transcription of *sim* in single rows of cells next to the mesoderm (mesectoderm) (Morel and Schweisguth 2000).

In the absence of the *Brd* complex, in which *Oche*, *Tom*, *BobA*, *BobB*, and *BobC* are clustered, the active endocytosis of Dl is observed in the entire embryo, indicating that the *Brd* family genes normally inhibit Neur activity in the dorsal region of the embryo (Bardin and Schweisguth 2006). Under the *Brd*-deleted condition, the *sim* expression is expanded (Bardin and Schweisguth 2006). To regulate *sim* expression, Brd proteins bind to Neur and interfere with the physical interaction between Neur and Dl (Lai *et al.* 2001; Bardin and Schweisguth 2006). However, unlike this mechanism

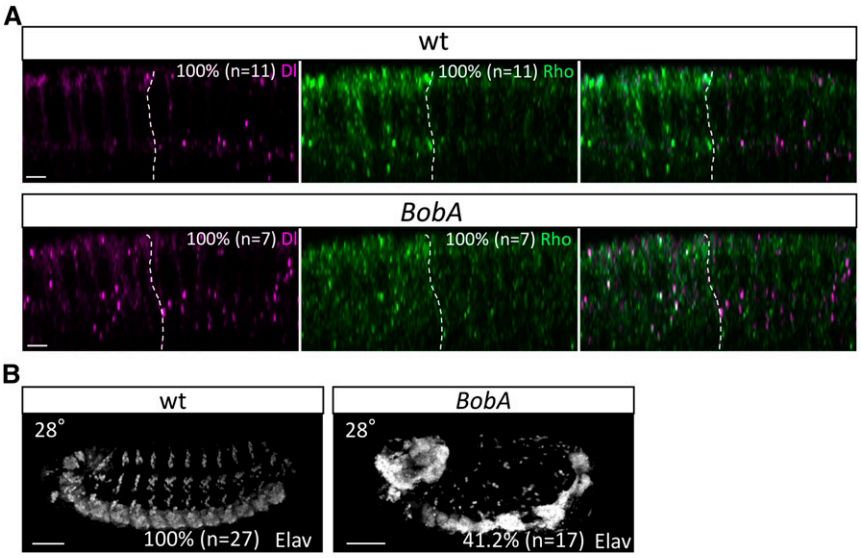

Figure 8 Dl recycling and Notch signaling are hyperactivated in the neuroectoderm of the *BobA* mutant. (A) Subcellular localization of Dl (magenta, left, and right panels) and Rhomboid (Rho) (green, middle, and right panels), a neuroectoderm marker, in wild-type (wt) or $BobA^1/BobA^1$ (*BobA*) embryos at stage 5. Boundary between the neuroectoderm and mesoderm is indicated by a white broken line, and the regions left (Rho-positive) and right (Rho-negative) of the broken lines are neuroectoderm and mesoderm, respectively. The percentage of embryos showing the represented phenotype is indicated at the upper right. The number of embryos examined is in parentheses. Bar, 5 μm. (B) Lateral views of wild-type (wt) and $BobA^1/BobA^1$ (*BobA*) embryos cultured at 28° and immunostained with a neuron-specific (anti-Elav) antibody at stage 13–14. Percentage of embryos showing the represented phenotype in each panel is shown at the bottom right, and the number of embryos examined is in parentheses. Bar, 50 μm.

of mesectoderm specification, the contribution of the Dl-Neur-BobA pathway to the regulation of Notch signaling during neuroblast segregation in the neuroectoderm has not been well studied. In the current study, we found that the neurogenic phenotype associated with the *pcx* mutation was dominantly enhanced by *neur* and *Dl* and suppressed by *BobA*. Consistent with these observations in $pcx/+^{m}$; $BobA^1/+$ embryos, Dl-containing vesicles were increased in the neuroectoderm of $BobA^1$ homozygous embryos, as well as in their dorsal side (Figure 8A). Moreover, we found that *BobA* homozygotes exhibited an anti-neurogenic phenotype at 28°, implying that Notch signaling was augmented during neuroblast segregation in these embryos (Figure 8B). Thus, our results suggest that the Dl-Neur-BobA pathway also functions in the regulation of Notch signaling during neuroblast segregation in the neuroectoderm.

Although the Dl endocytosis was hyperactivated in the neuroectoderm of $BobA^1$ mutant embryos, we did not observe an attenuation of Dl endocytosis even in the complete absence of *pcx* function (pcx^{mz} embryo) (Figure 7). In addition, we did not observe synergistic effects between *pcx* and *BobA* on the Dl endocytosis (Figure 8). Therefore, at this point, it is unclear whether Pcx has a direct role in the Dl-Neur-BobA pathway. We are currently investigating the potential connections between Pcx and Dl endocytosis.

lov transcribed in the early embryo may contribute to the activation of Notch signaling during neuroblast segregation

In this study, we identified the *lov* gene as a potential component of the Notch signaling pathway for the first time. *lov* encodes a Bric-a-Brac/Tramtrack/Broad/Pox virus and zinc finger (BTB/POZ) domain-containing transcription factor and is expressed in various neurons of the CNS and PNS and in the trachea during *Drosophila* development (Albagli *et al.* 1995; Armstrong *et al.* 2006). A loss-of-function mutant of *lov* demonstrates multiple behavioral defects in the larval and adult stages, including gravity sensing (Bjorum *et al.* 2013). These behavioral defects were previously attributed to the abnormal specifications of neurons, given that an absence of *lov* expression in a subset of neurons in mutants of a particular *lov* allele was correlated with the behavioral defects (Bjorum *et al.* 2013). The expression of *lov* was also observed in specific cells of the CNS midline in embryos (Wheeler *et al.* 2008). Notably, Notch signaling regulates gene expression in these CNS midline cells, which defines the fates of these cells (Wheeler *et al.* 2008). However, a detailed analysis of *lov* expression revealed that the *lov* gene is not a target of Notch signaling, at least in the ventral unpaired median neurons of the CNS midline (Wheeler *et al.* 2008). Although it is still possible that *lov* is involved in Notch signaling activation as a component of the pathway, the contribution of *lov* to Notch signaling appears to be highly context-dependent, redundant, or subtle, because the defects in the cell-fate specification of neurons found in *lov* mutants are much milder than those of classic Notch pathway genes (Bjorum *et al.* 2013).

It is reported that the expression of *lov* begins in the cellular blastoderm stage and continues during the development of the CNS and PNS (Kearney *et al.* 2004; Weiszmann *et al.* 2009). Furthermore, the Lov protein is detected in the neuroectoderm during the stage of neuroblast segregation, as well as in other parts of embryos (Bjorum *et al.* 2013). Therefore, *lov* may control the transcription of genes involved in Notch signaling during the periods of neuroblast segregation through lateral inhibition, although this possibility remains to be investigated. In any case, we speculate that the function of *lov* is not essential for Notch signaling during neuroblast segregation, given that *lov* homozygous embryos did not exhibit a neurogenic phenotype (data not shown). In addition, a maternal expression of *lov* was not observed, suggesting that *lov* does not have a maternal function (Coté *et al.* 1987). Therefore, it is unlikely that *lov* plays an indispensable

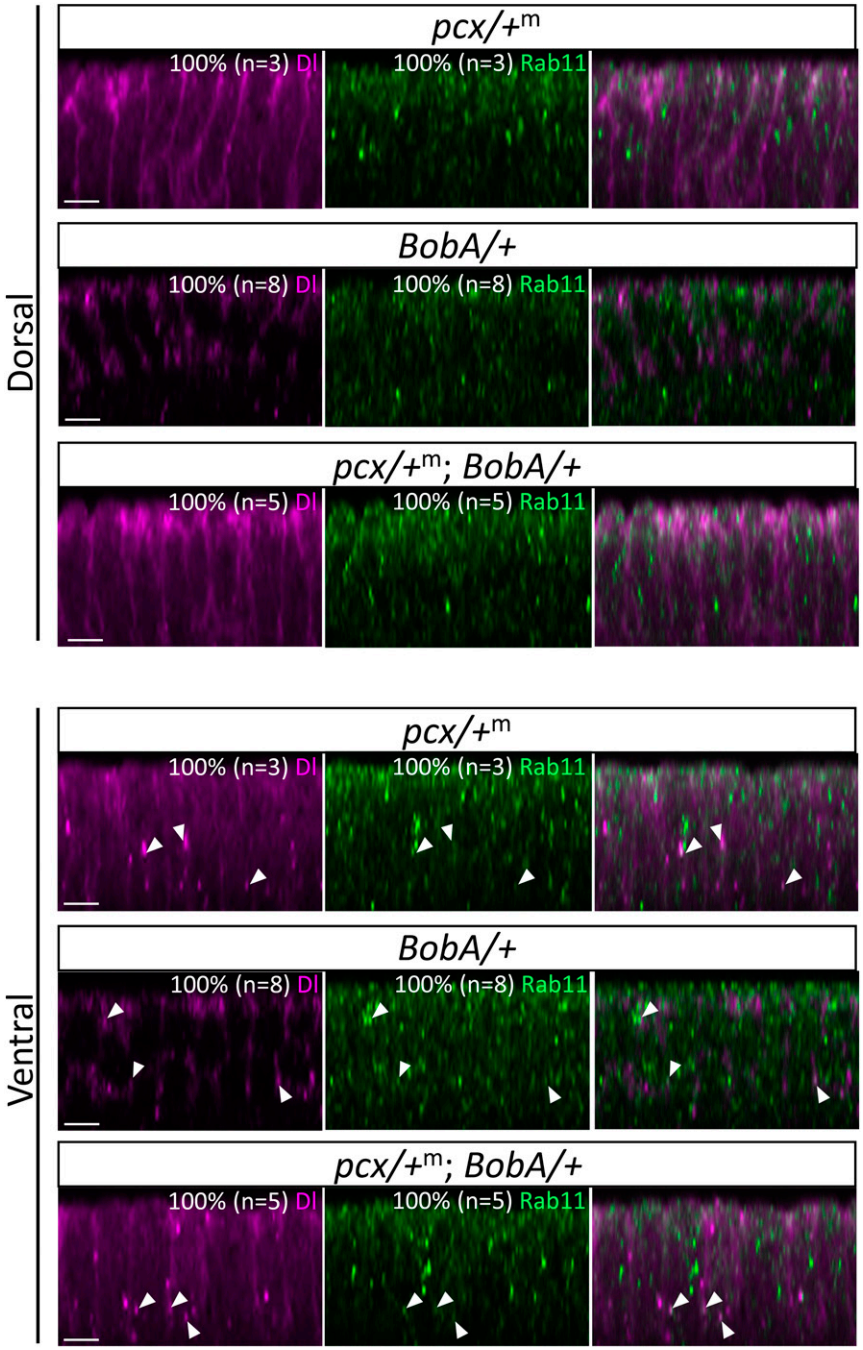

Figure 9 No synergistic interaction between *pcx*/+^{m} and *BobA*/+ in the Dl-trafficking phenotype. Subcellular localization of Dl (magenta, left, and right panels) and Rab11 (green, middle and right panels), a marker of recycling endosomes, in the dorsal (upper panels) and ventral (lower panels) epithelium of *pcx*/+^{m}, *BobA*/+, and *pcx*/+^{m}; *BobA*/+ embryos at stage 5. Right panels are merged images of the left and middle panels. White arrowheads indicate vesicles where Dl and Rab11 are colocalized. Percentage of embryos showing the represented phenotype is indicated at the upper right. The number of embryos examined is in parentheses. Bar, 5 μm.

role in lateral inhibition in the embryo, although our results suggest that it makes some contribution to it.

A novel role of Nsf2 supports the contribution of Pcx to ER homeostasis

In this study, we identified *Nsf2* as a dominant suppressor of *pcx*. *Drosophila* has two *Nsf* genes, *comatose* (*Nsf1*) and *Nsf2* (Pallanck *et al.* 1995a). The *Nsf* genes encode homohexameric AAA ATPases that are involved in the membrane fusion required for the transfer of membrane vesicles from one membrane compartment to another (Wilson *et al.* 1989; Söllner *et al.* 1993a). *Nsf1* is mainly expressed in neurons (Ordway *et al.* 1994), and its loss causes a disruption in synaptic transmission (Pallanck *et al.* 1995b; Gokhale *et al.* 2015). To ensure the specificity of membrane fusion, SNARE proteins on vesicles and target membranes form a tight complex (Söllner *et al.* 1993a). In this process, Nsf promotes the dissociation of SNARE complexes once membrane fusion has been completed, using ATP hydrolysis as the energy source (Söllner *et al.* 1993a). The dissociation of SNAREs is required for their recycling for further rounds of membrane fusion events (Söllner *et al.* 1993b). Thus, the absence of Nsf results in an attenuation of membrane trafficking (Beckers *et al.* 1989). These studies suggested that *Nsf1* functions to

disassemble SNARE complexes after vesicle docking, which is required to maintain the readily releasable pool of synaptic vesicles (Muller *et al.* 2002; Gokhale *et al.* 2015).

On the other hand, *Nsf2* is broadly expressed in embryonic and imaginal tissues, as well as in the nervous system (Boulianne and Trimble 1995). Therefore, *Nsf2* is likely to encode an Nsf isoform that contributes to vesicular trafficking in non-neuronal cells, including the neuroectoderm of the embryo (Boulianne and Trimble 1995). It was previously shown that the expression of a dominant-negative *Nsf2* ($Nsf2^{E/Q}$) suppresses Notch signaling in wing imaginal discs (Stewart *et al.* 2001). Genetic interaction between $Nsf2^{E/Q}$ and mutants of other genes encoding Notch-signaling components, including *Dl*, *Serrate*, *fringe*, and *bib*, has also been reported (Stewart *et al.* 2001). Notably, *bib* was also identified as a dominant enhancer of the $pcx/+^{m}$ lethality in the present study (Figure 4B and Figure S1). In addition, it was shown that Notch protein accumulates in the intracellular vesicles in epithelial cells misexpressing $Nsf2^{E/Q}$ (Stewart *et al.* 2001). The contribution of *Nsf2* to Notch signaling was further supported by the identification of *Nsf2* as a dominant enhancer of *Presenilin* hypomorphic mutants (Mahoney *et al.* 2006). These results all suggested that *Nsf2* positively contributes to Notch signaling (Mahoney *et al.* 2006). In contrast, in our screen, *Nsf2* was identified as a suppressor of *pcx*, demonstrating that the wild-type *Nsf2* gene suppresses Notch signaling activity under the conditions of our experiment. Thus, we speculate that *Nsf2* may have different roles in Notch signaling between imaginal tissues and embryonic neuroectoderm, which has not been noted before. This idea is consistent with the finding that various sets of SNAREs control the membrane fusion of different intracellular compartments under the control of an Nsf protein (Söllner *et al.* 1993b).

Furthermore, we previously reported that the ER is enlarged in a subset of cells in pcx^{mz} embryos (Yamakawa *et al.* 2012). In mammalian and yeast cells, Nsf is involved in ER membrane fusion and required for ER reassembly (Uchiyama *et al.* 2002; Kano *et al.* 2005). Thus, given that the ER enlargement in the absence of *pcx* function may be due to excessive assembly of the ER, a loss-of-function mutation of *Nsf2* may reduce the excess ER reassembly occurring in the absence of *pcx*. This scenario is consistent with the behavior of *Nsf2* as a dominant suppressor of $pcx/+^{m}$ lethality. This mechanism is currently under active investigation in our laboratory.

The genetic screens performed in the current study identified dominant modifiers of the cold-sensitive lethality associated with a *pcx* mutation condition. In particular, although the genetic interactions of *pcx* with *neur* or *BobA* may not reflect a direct relationship with respect to the regulation of Dl endocytosis, the results obtained from our genetic screens revealed intimate relationships between Pcx and the Notch signaling pathway and implied a close relationship between *pcx* function and vesicular transport during neuroblast segregation in the neuroectoderm. Furthermore, our analysis uncovered a potential role of *lov* and a previously unknown function of *Nsf2* in Notch signaling. There results contribute to our understanding of the complex regulation of Notch signaling.

Acknowledgments

We thank Kathleen Beckingham and Markus Noll for providing fly stocks. We thank Akira Nakamura, Ethan Bier and Spyros Artavanis-Tsakonas for providing antibodies. We also thank the KYOTO Stock Center (Kyoto), the Bloomington Drosophila Stock Center (Indiana), and the Developmental Studies Hybridoma Bank (University of Iowa). This work was supported by JSPS KAKENHI grant number JP25840074 and by a Japan Prize Foundation 2014 grant.

Literature Cited

Albagli, O., P. Dhordain, C. Deweindt, G. Lecocq, and D. Leprince, 1995 The BTB/POZ domain: a new protein-protein interaction motif common to DNA- and actin-binding proteins. Cell Growth Differ. 6: 1193–1198.

Armstrong, J. D., M. J. Texada, R. Munjaal, D. A. Baker, and K. M. Beckingham, 2006 Gravitaxis in Drosophila melanogaster: a forward genetic screen. Genes Brain Behav. 5: 222–239. https://doi.org/10.1111/j.1601-183X.2005.00154.x

Artavanis-Tsakonas, S., K. Matsuno, and M. E. Fortini, 1995 Notch signaling. Science 268: 225–232.

Artavanis-Tsakonas, S., M. D. Rand, and R. J. Lake, 1999 Notch signaling: cell fate control and signal integration in development. Science 284: 770–776.

Ashburner, M., 1989 *Drosophila: A Laboratory Manual*. Cold Spring Harbor Laboratory Press, Cold Spring Harbor, NY.

Bailey, A. M., and J. W. Posakony, 1995 Suppressor of hairless directly activates transcription of enhancer of split complex genes in response to Notch receptor activity. Genes Dev. 9: 2609–2622.

Bardin, A. J., and F. Schweisguth, 2006 Bearded family members inhibit Neuralized-mediated endocytosis and signaling activity of Delta in Drosophila. Dev. Cell 10: 245–255. https://doi.org/10.1016/j.devcel.2005.12.017

Bechstedt, S., J. T. Albert, D. P. Kreil, T. Müller-Reichert, M. C. Göpfert *et al.*, 2010 A doublecortin containing microtubule-associated protein is implicated in mechanotransduction in Drosophila sensory cilia. Nat. Commun. 1: 11. https://doi.org/10.1038/ncomms1007

Beckers, C. J., M. R. Block, B. S. Glick, J. E. Rothman, and W. E. Balch, 1989 Vesicular transport between the endoplasmic reticulum and the Golgi stack requires the NEM-sensitive fusion protein. Nature 339: 397–398. https://doi.org/10.1038/339397a0

Bessho, Y., and R. Kageyama, 2003 Oscillations, clocks and segmentation. Curr. Opin. Genet. Dev. 13: 379–384.

Bjorum, S. M., R. A. Simonette, R. Alanis, Jr., J. E. Wang, B. M. Lewis *et al.*, 2013 The Drosophila BTB domain protein jim lovell has roles in multiple larval and adult behaviors. PLoS One 8: e61270. https://doi.org/10.1371/journal.pone.0061270

Bopp, D., L. R. Bell, T. W. Cline, and P. Schedl, 1991 Developmental distribution of female-specific sex-lethal proteins in Drosophila melanogaster. Genes Dev. 5: 403–415.

Boulianne, G. L., and W. S. Trimble, 1995 Identification of a second homolog of N-ethylmaleimide-sensitive fusion protein that is expressed in the nervous system and secretory tissues of Drosophila. Proc. Natl. Acad. Sci. USA 92: 7095–7099.

Bray, S. J., 2016 Notch signalling in context. Nat. Rev. Mol. Cell Biol. 17: 722–735. https://doi.org/10.1038/nrm.2016.94

Bruckner, K., L. Perez, H. Clausen, and S. Cohen, 2000 Glycosyltransferase activity of Fringe modulates Notch-Delta interactions. Nature 406: 411–415 (erratum: Nature 407: 654). https://doi.org/10.1038/35019075

Cau, E., and P. Blader, 2009 Notch activity in the nervous system: to switch or not switch? Neural Dev. 4: 36. https://doi.org/10.1186/1749-8104-4-36

Chanet, S., and F. Schweisguth, 2012 Regulation of epithelial polarity by the E3 ubiquitin ligase Neuralized and the Bearded inhibitors in Drosophila. Nat. Cell Biol. 14: 467–476. https://doi.org/10.1038/ncb2481

Cook, R. K., S. J. Christensen, J. A. Deal, R. A. Coburn, M. E. Deal *et al.*, 2012 The generation of chromosomal deletions to provide extensive coverage and subdivision of the Drosophila melanogaster genome. Genome Biol. 3: R21. https://doi.org/10.1186/gb-2012-13-3-r21

Coté, S., A. Preiss, J. Haller, R. Schuh, A. Kienlin *et al.*, 1987 The gooseberry-zipper region of Drosophila: five genes encode different spatially restricted transcripts in the embryo. EMBO J. 6: 2793–2801.

De Celis, J. F., and A. García-Bellido, 1994 Roles of the Notch gene in Drosophila wing morphogenesis. Mech. Dev. 46: 109–122.

Dellinger, B., R. Felling, and R. W. Ordway, 2000 Genetic modifiers of the Drosophila NSF mutant, comatose, include a temperature-sensitive paralytic allele of the calcium channel alpha1-subunit gene, cacophony. Genetics 155: 203–211.

De Renzis, S., J. Yu, R. Zinzen, and E. Wieschaus, 2006 Dorsal-ventral pattern of Delta trafficking is established by a Snail-Tom-Neuralized pathway. Dev. Cell 10: 257–264. https://doi.org/10.1016/j.devcel.2006.01.011

Doherty, D., L. Y. Jan, and Y. N. Jan, 1997 The Drosophila neurogenic gene big brain, which encodes a membrane-associated protein, acts cell autonomously and can act synergistically with Notch and Delta. Development 124: 3881–3893.

Ellisen, L. W., J. Bird, D. C. West, A. L. Soreng, T. C. Reynolds *et al.*, 1991 TAN-1, the human homolog of the Drosophila notch gene, is broken by chromosomal translocations in T lymphoblastic neoplasms. Cell 66: 649–661.

Emery, G., A. Hutterer, D. Berdnik, B. Mayer, F. Wirtz-Peitz *et al.*, 2005 Asymmetric Rab 11 endosomes regulate delta recycling and specify cell fate in the Drosophila nervous system. Cell 122: 763–773. https://doi.org/10.1016/j.cell.2005.08.017

Fehon, R. G., P. J. Kooh, I. Rebay, C. L. Regan, T. Xu *et al.*, 1990 Molecular interactions between the protein products of the neurogenic loci Notch and Delta, two EGF-homologous genes in Drosophila. Cell 61: 523–534.

Gilbert, T. L., B. A. Haldeman, E. Mulvihill, and P. J. O'Hara, 1992 A mammalian homologue of a transcript from the Drosophila pecanex locus. J. Neurogenet. 8: 181–187.

Go, M. J., D. S. Eastman, and S. Artavanis-Tsakonas, 1998 Cell proliferation control by Notch signaling in Drosophila development. Development 125: 2031–2040.

Gokhale, A., A. P. Mullin, S. A. Zlatic, C. A. Easley, IV, M. E. Merritt *et al.*, 2015 The N-ethylmaleimide-sensitive factor and dysbindin interact to modulate synaptic plasticity. J. Neurosci. 35: 7643–7653. https://doi.org/10.1523/JNEUROSCI.4724-14.2015

Guruharsha, K. G., M. W. Kankel, and S. Artavanis-Tsakonas, 2012 The Notch signalling system: recent insights into the complexity of a conserved pathway. Nat. Rev. Genet. 13: 654–666. https://doi.org/10.1038/nrg3272

He, H., and M. Noll, 2013 Differential and redundant functions of gooseberry and gooseberry neuro in the central nervous system and segmentation of the Drosophila embryo. Dev. Biol. 382: 209–223. https://doi.org/10.1016/j.ydbio.2013.05.017

Hori, K., A. Sen, and S. Artavanis-Tsakonas, 2013 Notch signaling at a glance. J. Cell Sci. 126: 2135–2140. https://doi.org/10.1242/jcs.127308

Ishio, A., T. Sasamura, T. Ayukawa, J. Kuroda, H. O. Ishikawa *et al.*, 2015 O-fucose monosaccharide of Drosophila Notch has a temperature-sensitive function and cooperates with O-glucose glycan in Notch transport and Notch signaling activation. J. Biol. Chem. 290: 505–519. https://doi.org/10.1074/jbc.M114.616847

John, G. R., S. L. Shankar, B. Shafit-Zagardo, A. Massimi, S. C. Lee *et al.*, 2002 Multiple sclerosis: re-expression of a developmental pathway that restricts oligodendrocyte maturation. Nat. Med. 8: 1115–1121. https://doi.org/10.1038/nm781

Joutel, A., K. Vahedi, C. Corpechot, A. Troesch, H. Chabriat *et al.*, 1997 Strong clustering and stereotyped nature of Notch3 mutations in CADASIL patients. Lancet 350: 1511–1515. https://doi.org/10.1016/S0140-6736(97)08083-5

Kano, F., H. Kondo, A. Yamamoto, Y. Kaneko, K. Uchiyama *et al.*, 2005 NSF/SNAPs and p97/p47/VCIP135 are sequentially required for cell cycle-dependent reformation of the ER network. Genes Cells 10: 989–999. https://doi.org/10.1111/j.1365-2443.2005.00894.x

Kaufman, R. J., 1999 Stress signaling from the lumen of the endoplasmic reticulum: coordination of gene transcriptional and translational controls. Genes Dev. 13: 1211–1233.

Kaufmann, N., J. C. Mathai, W. G. Hill, J. A. Dow, M. L. Zeidel *et al.*, 2005 Developmental expression and biophysical characterization of a Drosophila melanogaster aquaporin. Am. J. Physiol. Cell Physiol. 289: C397–C407. https://doi.org/10.1152/ajpcell.00612.2004

Kearney, J. B., S. R. Wheeler, P. Estes, B. Parente, and S. T. Crews, 2004 Gene expression profiling of the developing Drosophila CNS midline cells. Dev. Biol. 275: 473–492. https://doi.org/10.1016/j.ydbio.2004.08.047

Kidd, S., and T. Lieber, 2002 Furin cleavage is not a requirement for Drosophila Notch function. Mech. Dev. 115: 41–51.

Kim, J., A. Sebring, J. J. Esch, M. E. Kraus, K. Vorwerk *et al.*, 1996 Integration of positional signals and regulation of wing formation and identity by Drosophila vestigial gene. Nature 382: 133–138. https://doi.org/10.1038/382133a0

Kopan, R., and M. X. Ilagan, 2009 The canonical Notch signaling pathway: unfolding the activation mechanism. Cell 137: 216–233. https://doi.org/10.1016/j.cell.2009.03.045

Kopczynski, C. C., A. K. Alton, K. Fechtel, P. J. Kooh, and M. A. Muskavitch, 1988 Delta, a Drosophila neurogenic gene, is transcriptionally complex and encodes a protein related to blood coagulation factors and epidermal growth factor of vertebrates. Genes Dev. 2: 1723–1735.

Kozlova, T., G. V. Pokholkova, G. Tzertzinis, J. D. Sutherland, I. F. Zhimulev *et al.*, 1998 Drosophila hormone receptor 38 functions in metamorphosis: a role in adult cuticle formation. Genetics 149: 1465–1475.

LaBonne, S. G., I. Sunitha, and A. P. Mahowald, 1989 Molecular genetics of pecanex, a maternal-effect neurogenic locus of Drosophila melanogaster that potentially encodes a large transmembrane protein. Dev. Biol. 136: 1–16.

Lai, E. C., R. Bodner, J. Kavaler, G. Freschi, and J. W. Posakony, 2000 Antagonism of Notch signaling activity by members of a novel protein family encoded by the bearded and enhancer of split gene complexes. Development 127: 291–306.

Lai, E. C., G. A. Deblandre, C. Kintner, and G. M. Rubin, 2001 Drosophila neuralized is a ubiquitin ligase that promotes the internalization and degradation of delta. Dev. Cell 1: 783–794.

Lake, R. J., L. M. Grimm, A. Veraksa, A. Banos, and S. Artavanis-Tsakonas, 2009 In vivo analysis of the Notch receptor S1 cleavage. PLoS One 4: e6728. https://doi.org/10.1371/journal.pone.0006728

Le Borgne, R., S. Remaud, S. Hamel, and F. Schweisguth, 2005 Two distinct E3 ubiquitin ligases have complementary functions in the regulation of delta and serrate signaling in Drosophila. PLoS Biol. 3: e96. https://doi.org/10.1371/journal.pbio.0030096

Le Bras, S., N. Loyer, and R. Le Borgne, 2011 The multiple facets of ubiquitination in the regulation of Notch signaling pathway. Traffic 12: 149–161. https://doi.org/10.1111/j.1600-0854.2010.01126.x

Lehmann, R., U. Dietrich, F. Jimenez, and J. A. Campos-Ortega, 1981 Mutations of early neurogenesis in Drosophila. Rouxs Arch. Dev. Biol. 190: 226–229.

Lehmann, R., F. Jimenez, U. Dietrich, and J. A. Campos-Ortega, 1983 On the phenotype and development of mutants of early neurogenesis in Drosophila melanogaster. Rouxs Arch. Dev. Biol. 192: 62–74.

Leonardi, J., R. Fernandez-Valdivia, Y. D. Li, A. A. Simcox, and H. Jafar-Nejad, 2011 Multiple O-glucosylation sites on Notch function as a buffer against temperature-dependent loss of signaling. Development 138: 3569–3578. https://doi.org/10.1242/dev.068361

Leviten, M. W., and J. W. Posakony, 1996 Gain-of-function alleles of Bearded interfere with alternative cell fate decisions in Drosophila adult sensory organ development. Dev. Biol. 176: 264–283. https://doi.org/10.1006/dbio.1996.0133

Li, L., I. D. Krantz, Y. Deng, A. Genin, A. B. Banta *et al.*, 1997 Alagille syndrome is caused by mutations in human Jagged1, which encodes a ligand for Notch1. Nat. Genet. 16: 243–251. https://doi.org/10.1038/ng0797-243

Lindsay, H. A., R. Baines, R. ffrench-Constant, K. Lilley, H. T. Jacobs *et al.*, 2008 The dominant cold-sensitive Out-cold mutants of Drosophila melanogaster have novel missense mutations in the voltage-gated sodium channel gene paralytic. Genetics 180: 873–884. https://doi.org/10.1534/genetics.108.090951

Logeat, F., C. Bessia, C. Brou, O. LeBail, S. Jarriault *et al.*, 1998 The Notch1 receptor is cleaved constitutively by a furin-like convertase. Proc. Natl. Acad. Sci. USA 95: 8108–8112.

Mahoney, M. B., A. L. Parks, D. A. Ruddy, S. Y. Tiong, H. Esengil *et al.*, 2006 Presenilin-based genetic screens in Drosophila melanogaster identify novel Notch pathway modifiers. Genetics 172: 2309–2324. https://doi.org/10.1534/genetics.104.035170

Meloty-Kapella, L., B. Shergill, J. Kuon, E. Botvinick, and G. Weinmaster, 2012 Notch ligand endocytosis generates mechanical pulling force dependent on dynamin, epsins, and actin. Dev. Cell 22: 1299–1312. https://doi.org/10.1016/j.devcel.2012.04.005

Mohler, D., and A. Carroll, 1984 Report of new mutants. Drosoph. Inf. Serv. 60: 236–241.

Mohler, J. D., 1977 Developmental genetics of the Drosophila egg. I. Identification of 59 sex-linked cistrons with maternal effects on embryonic development. Genetics 85: 259–272.

Morel, V., and F. Schweisguth, 2000 Repression by suppressor of hairless and activation by Notch are required to define a single row of single-minded expressing cells in the Drosophila embryo. Genes Dev. 14: 377–388.

Muller, J. M., J. Shorter, R. Newman, K. Deinhardt, Y. Sagiv *et al.*, 2002 Sequential SNARE disassembly and GATE-16-GOS-28 complex assembly mediated by distinct NSF activities drives Golgi membrane fusion. J. Cell Biol. 157: 1161–1173. https://doi.org/10.1083/jcb.200202082

Mumm, J. S., and R. Kopan, 2000 Notch signaling: from the outside in. Dev. Biol. 228: 151–165. https://doi.org/10.1006/dbio.2000.9960

Nicolas, M., A. Wolfer, K. Raj, J. A. Kummer, P. Mill *et al.*, 2003 Notch1 functions as a tumor suppressor in mouse skin. Nat. Genet. 33: 416–421. https://doi.org/10.1038/ng1099

O'Connell, K. F., C. M. Leys, and J. G. White, 1998 A genetic screen for temperature-sensitive cell-division mutants of Caenorhabditis elegans. Genetics 149: 1303–1321.

Ordway, R., L. Pallanck, and B. Ganetzky, 1994 Neurally expressed Drosophila genes encoding homologs of the NSF and SNAP secretory proteins. Proc. Natl. Acad. Sci. USA 91: 5715–5719.

Pallanck, L., R. W. Ordway, M. Ramaswami, W. Y. Chi, K. S. Krishnan *et al.*, 1995a Distinct roles for N-ethylmaleimide-sensitive fusion protein (NSF) suggested by the identification of a second Drosophila NSF homolog. J. Biol. Chem. 270: 18742–18744.

Pallanck, L., R. W. Ordway, and B. Ganetzky, 1995b A Drosophila NSF mutant. Nature 376: 25. https://doi.org/10.1038/376025a0

Palmeirim, I., D. Henrique, D. Ish-Horowicz, and O. Pourquié, 1997 Avian hairy gene expression identifies a molecular clock linked to vertebrate segmentation and somitogenesis. Cell 91: 639–648.

Park, J. S., S. R. Kim, S. Y. Park, D. J. Yang, S. H. Lee *et al.*, 2008 Big brain, a Drosophila homologue of mammalian aquaporin, is regulated by the DRE/DREF system. Biochim. Biophys. Acta 1779: 789–796. https://doi.org/10.1016/j.bbagrm.2008.07.015

Parks, A. L., K. R. Cook, M. Belvin, N. A. Dompe, R. Fawcett *et al.*, 2004 Systematic generation of high-resolution deletion coverage of the Drosophila melanogaster genome. Nat. Genet. 36: 288–292. https://doi.org/10.1038/ng1312

Pavlopoulos, E., C. Pitsouli, K. M. Klueg, M. A. Muskavitch, N. K. Moschonas *et al.*, 2001 Neuralized encodes a peripheral membrane protein involved in delta signaling and endocytosis. Dev. Cell 1: 807–816.

Perrimon, N., L. Engstrom, and A. P. Mahowald, 1984 Developmental genetics of the 2E-F region of the Drosophila X chromosome: a region rich in "developmentally important" genes. Genetics 108: 559–572.

Rebay, I., R. J. Fleming, R. G. Fehon, L. Cherbas, P. Cherbas *et al.*, 1991 Specific EGF repeats of Notch mediate interactions with Delta and Serrate: implications for Notch as a multifunctional receptor. Cell 67: 687–699.

Rhyu, M. S., L. Y. Jan, and Y. N. Jan, 1994 Asymmetric distribution of numb protein during division of the sensory organ precursor cell confers distinct fates to daughter cells. Cell 76: 477–491.

Shellenbarger, D. L., and J. D. Mohler, 1978 Temperature-sensitive periods and autonomy of pleiotropic effects of l(1)Nts1, a conditional notch lethal in Drosophila. Dev. Biol. 62: 432–446.

Shimizu, H., S. A. Woodcock, M. B. Wilkin, B. Trubenová, N. A. Monk *et al.*, 2014 Compensatory flux changes within an endocytic trafficking network maintain thermal robustness of Notch signaling. Cell 157: 1160–1174. https://doi.org/10.1016/j.cell.2014.03.050

Simpson, P., 1990 Lateral inhibition and the development of the sensory bristles of the adult peripheral nervous system of Drosophila. Development 109: 509–519.

Söllner, T., S. W. Whiteheart, M. Brunner, H. Erdjument-Bromage, S. Geromanos *et al.*, 1993a SNAP receptors implicated in vesicle targeting and fusion. Nature 362: 318–324. https://doi.org/10.1038/362318a0

Söllner, T., M. K. Bennett, S. W. Whiteheart, R. H. Scheller, and J. E. Rothman, 1993b A protein assembly-disassembly pathway in vitro that may correspond to sequential steps of synaptic vesicle docking, activation and fusion. Cell 75: 409–418.

Stephenson, N. L., and J. M. Avis, 2012 Direct observation of proteolytic cleavage at the S2 site upon forced unfolding of the Notch negative regulatory region. Proc. Natl. Acad. Sci. USA 109: E2757–E2765. https://doi.org/10.1073/pnas.1205788109

Stewart, B. A., M. Mohtashami, L. Zhou, W. S. Trimble, and G. L. Boulianne, 2001 SNARE-dependent signaling at the Drosophila

wing margin. Dev. Biol. 234: 13–23. https://doi.org/10.1006/dbio.2001.0228

St Johnston, D., 2002 The art and design of genetic screens: Drosophila melanogaster. Nat. Rev. Genet. 3: 176–188. https://doi.org/10.1038/nrg751

Struhl, G., K. Fitzgerald, and I. Greenwald, 1993 Intrinsic activity of the Lin12 and Notch intracellular domains in vivo. Cell 74: 331–345.

Sturtevant, M. A., M. Roark, J. W. O'Neill, B. Biehs, N. Colley *et al.*, 1996 The Drosophila rhomboid protein is concentrated in patches at the apical cell surface. Dev. Biol. 174: 298–309. https://doi.org/10.1006/dbio.1996.0075

Tanaka, T., and A. Nakamura, 2008 The endocytic pathway acts downstream of Oskar in Drosophila germ plasm assembly. Development 135: 1107–1117. https://doi.org/10.1242/dev.017293

Thibault, S. T., M. A. Singer, W. Y. Miyazaki, B. Milash, N. A. Dompe *et al.*, 2004 A complementary transposon tool kit for Drosophila melanogaster using P and piggyBac. Nat. Genet. 36: 283–287. https://doi.org/10.1038/ng1314

Uchiyama, K., E. Jokitalo, F. Kano, M. Murata, X. Zhang *et al.*, 2002 VCIP135, a novel essential factor for p97/p47-mediated membrane fusion, is required for Golgi and ER assembly in vivo. J. Cell Biol. 159: 855–866. https://doi.org/10.1083/jcb.200208112

Vässin, H., and J. A. Campos-Ortega, 1987 Genetic analysis of Delta, a neurogenic gene of Drosophila melanogaster. Genetics 116: 433–445.

Vässin, H., K. A. Bremer, E. Knust, and J. A. Campos-Ortega, 1987 The neurogenic Gene Delta of Drosophila melanogaster is expressed in neurogenic territories and encodes a putative transmembrane protein with EGF-like repeats. EMBO J. 6: 3431–3440.

Wang, W., and G. Struhl, 2004 Drosophila Epsin mediates a select endocytic pathway that DSL ligands must enter to activate Notch. Development 131: 5367–5380. https://doi.org/10.1242/dev.01413

Wang, W., and G. Struhl, 2005 Distinct roles for Mind bomb, Neuralized and Epsin in mediating DSL endocytosis and signaling in Drosophila. Development 132: 2883–2894. https://doi.org/10.1242/dev.01860

Weiszmann, R., A. S. Hammonds, and S. E. Celniker, 2009 Determination of gene expression patterns using high-throughput RNA in situ hybridization to whole-mount Drosophila embryos. Nat. Protoc. 4: 605–618. https://doi.org/10.1038/nprot.2009.55

Wharton, K. A., K. M. Johansen, T. Xu, and S. Artavanis-Tsakonas, 1985 Nucleotide sequence from the neurogenic locus notch implies a gene product that shares homology with proteins containing EGF-like repeats. Cell 43: 567–581.

Wheeler, S. R., S. B. Stagg, and S. T. Crews, 2008 Multiple Notch signaling events control Drosophila CNS midline neurogenesis, gliogenesis and neuronal identity. Development 135: 3071–3079. https://doi.org/10.1242/dev.022343

Wilson, D. W., C. A. Wilcox, G. C. Flynn, E. Chen, W. J. Kuang *et al.*, 1989 A fusion protein required for vesicle-mediated transport in both mammalian cells and yeast. Nature 339: 355–359. https://doi.org/10.1038/339355a0

Yamakawa, T., K. Yamada, T. Sasamura, N. Nakazawa, M. Kanai *et al.*, 2012 Deficient Notch signaling associated with neurogenic pecanex is compensated for by the unfolded protein response in Drosophila. Development 139: 558–567. https://doi.org/10.1242/dev.073858

Young, R. S., A. C. Marques, C. Tibbit, W. Haerty, A. R. Bassett *et al.*, 2012 Identification and properties of 1,119 candidate lincRNA loci in the Drosophila melanogaster genome. Genome Biol. Evol. 4: 427–442. https://doi.org/10.1093/gbe/evs020

Communicating editor: M. Rose